

Non-Cold Dark Matter from Primordial Black Hole Evaporation

Iason Baldes,^a Quentin Decant,^a Deanna C. Hooper,^a
and Laura Lopez-Honorez^{ab}

^aService de Physique Théorique, CP225, Université Libre de Bruxelles, Bld du Triomphe, B-1050 Brussels, Belgium

^bTheoretische Natuurkunde, Vrije Universiteit Brussel and The International Solvay Institutes, Pleinlaan 2, B-1050 Brussels, Belgium

E-mail: iason.baldes@ulb.ac.be, quentin.decant@ulb.ac.be, deanna.hooper@ulb.be, llopezho@ulb.ac.be

Abstract. Dark matter coupled solely gravitationally can be produced through the decay of primordial black holes in the early universe. If the dark matter is lighter than the initial black hole temperature, it could be warm enough to be subject to structure formation constraints. In this paper we perform a more precise determination of these constraints. We first evaluate the dark matter phase-space distribution, without relying on the instantaneous decay approximation. We then interface this phase-space distribution with the Boltzmann code CLASS to extract the corresponding matter power spectrum, which we find to match closely those of warm dark matter models, albeit with a different dark matter mass. This mapping allows us to extract constraints from Lyman- α data without the need to perform hydrodynamical simulations. We robustly rule out the possibility, consistent with previous analytic estimates, of primordial black holes having come to dominate the energy density of the universe and simultaneously given rise to all the DM through their decay. Consequences and implications for dark radiation and leptogenesis are also briefly discussed.

Contents

1	Introduction	1
2	Black holes: origin and evaporation	2
3	Relic dark matter from evaporation	5
4	Non-cold dark matter phase-space distribution	8
4.1	Instantaneous reheating	9
4.2	Non-instantaneous reheating	10
4.3	NCDM phase-space distribution	11
5	The non-cold dark matter imprint	11
5.1	Estimate for the Lyman- α constraint	12
5.2	Lyman- α constraints from the transfer function	13
5.3	Contribution to ΔN_{eff}	15
6	Viable parameter space from cosmology	17
7	Leptogenesis from PBH evaporation	19
8	Conclusions	20
A	Greybody factors	22
B	Validity of instantaneous evaporation approximation	23
C	Changing the number of degrees of freedom	24
D	Radiation contributions	25

1 Introduction

Dark matter (DM) is a cornerstone of both modern cosmology and particle physics. Despite this, one of the most well-motivated candidates, the Weakly Interacting Massive Particle (WIMP), in which the DM is produced via freeze-out in the early universe, has thus far avoided detection [1]. Combined with possible cosmological failings of the standard cold dark matter (CDM) paradigm on small scales [2–4], this has reinvigorated interest in non-cold dark matter models (NCDM) [5], and alternative production mechanisms involving more feebly coupled DM candidates, see e.g. [6–9].

Another possibility is for DM to not be a particle, but rather a population of primordial black holes (PBHs). The early universe is thought to have undergone a period of inflation, diluting away any existing curvature, and along with it any matter or radiation. The inflaton field eventually decayed, reheating the universe, and imprinting its fluctuations on the radiation density. A large enough overdensity will collapse and form PBHs once the fluctuation re-enters the Hubble horizon [10, 11]. The PBHs, if massive enough to be stable on cosmological timescales, are a suitable DM candidate. This possibility, however, has been put under

pressure from various considerations, including accretion and subsequent energy injection into the CMB [12, 13], lensing observations [14], and constraints from star formation [15], meaning much of the possible mass range is disfavoured [16]. Nevertheless, this remains an active area of research with many constraints having recently been either tightened or re-evaluated entirely [17, 18].

Alternatively, the PBHs may be light enough to decay via Hawking radiation [19, 20] at an early enough epoch to avoid these constraints. Strong limits exist on PBHs which decay between big bang nucleosynthesis (BBN) and recombination from the observed yields of light elements [17, 21] and observations of CMB anisotropies [22–24], which may be further strengthened through the use of CMB spectral distortions [25, 26]. Early work on PBHs which decay before BBN focused on the possibility of the DM being composed of stable Planck scale remnants of the PBHs [27, 28]. Here we will instead assume the PBHs decay away completely, and consider particle DM candidates which – even if they only have gravitational interactions – can be produced through PBH decay [28–37]. This results in a tight relation between the initial PBH mass, the DM mass, the initial density fraction of the universe in PBHs, and T_{ev} , the temperature of the universe immediately after the PBHs evaporate.

In this paper we revisit the production of NCDM lighter than the initial black hole temperature at formation and explore the different bounds on such models; coming from inflation, BBN, the observed DM relic abundance, the effective number of relativistic degrees-of-freedom N_{eff} , and structure formation. For the first time, we will explore the full impact of the non-instantaneous evaporation of the PBHs on the resulting NCDM. To do this, we use the phase-space distribution of such models as an input for the Boltzmann code CLASS [38], which then allows us to extract the matter power spectrum, and thus the transfer function of these models compared to the standard Λ CDM case. This enables us in turn to constrain the model using the structure formation bounds from Lyman- α data [39–41].

This paper is organised as follows. In Sec. 2 we briefly introduce the context in which we consider PBH formation and their decay products. We go on in Sec. 3 to find the DM mass required for the PBH decay to produce the observed DM relic abundance. In Sec. 4 we derive the resulting non-cold phase-space density of the DM. In Sec. 5 we constrain the scenario from its effects on structure formation by calculating the power spectrum and comparing it with Lyman- α limits. Possible contributions to ΔN_{eff} are also discussed. The main results of our paper are presented in Sec. 6, which summarises the allowed parameter space of the model. We then make some comments regarding the consequences for leptogenesis in Sec. 7, before concluding in Sec. 8. We add further details on some of our calculations in the appendices. In particular, in App. A we discuss how a more detailed treatment of the greybody factors might affect our results, in App. B we address the validity of the instantaneous reheating assumption, in App. C we detail how changes in the number of degrees of freedom (dark or not) affect our results and, finally, in App. D we derive the expressions for ΔN_{eff} .

2 Black holes: origin and evaporation

A non-rotating BH with zero charge and temperature given by¹

$$T_{\text{BH}} = \frac{M_p^2}{8\pi M_{\text{BH}}}, \quad (2.1)$$

¹For a black hole in a stationary spacetime the temperature is defined as $T_{\text{BH}} = \kappa/2\pi$, with κ the surface gravity [42]. If the black hole is charged or rotating, its temperature will differ from eq. (2.1).

with the Planck mass $M_p = 1.22 \times 10^{19} \text{ GeV}$ and M_{BH} the BH mass, will emit particles of the j th species at an averaged rate per energy interval of:

$$\frac{dN_j}{dt dE} = \frac{g_j}{2\pi} \frac{\Gamma_j(E, M_{\text{BH}})}{\exp(E/T_{\text{BH}}) \pm 1}, \quad (2.2)$$

when considering fermion (+) or boson (−) emission, and g_j denotes the number of degrees of freedom (dof) of the species j , see e.g. [43, 44] for the more general case. The coefficients $\Gamma_j(E, M_{\text{BH}})$ are absorption probabilities, referred to as *greybody factors* [45], which depend on the energy of the particles, the mass of the BH, and the properties of the particle j . They can be obtained by computing the transmission coefficients of a wave of energy E between the BH horizon and spatial infinity, but they are non-trivial to evaluate (see, however, [46] for a new tool). They tend to $\Gamma_j(E, M_{\text{BH}}) = 27E^2 M_{\text{BH}}^2 / M_p^4$ in the high energy ($E \gg T_{\text{BH}}$) geometrical-optics limit, while they fall off more quickly as $E \rightarrow 0$, with higher spins producing stronger cutoffs [45]. Here in order to provide a self consistent analysis and simple analytic estimates, we make use of the geometrical-optics limit. We note, however, that this ignores small spin-dependent low- E suppressions of the spectrum, and as such will lead to a slight underestimation of the total portion of relativistic (high- E) particles as already mentioned in [33]. We provide more details on the expected effects of a detailed processing of greybody factors in App. A.

Within this context, combining eqs. (2.2) and (2.1), the emitted power implies that the BH mass decreases with time at a rate

$$\frac{dM_{\text{BH}}}{dt} = - \sum_j \int_0^\infty E \frac{dN_j}{dt dE} dE = -e_T \frac{M_p^4}{M_{\text{BH}}^2}, \quad (2.3)$$

where e_T is given by

$$e_T = \frac{27}{4} \frac{g_{*\text{BH}}}{30720\pi}. \quad (2.4)$$

Here we have introduced $g_{*\text{BH}}$, the total number of relativistic degrees of freedom (i.e. with $m_j < T_{\text{BH}}$) emitted by the BH. For definitiveness, in the following we will assume that the BH will emit a two-component fermionic DM particle with mass $m_{\text{DM}} < T_{\text{BH}}$ together with Standard Model (SM) particles. In particular, for BHs with a temperature above the approximate electroweak phase transition temperature, T_{EW} , the SM relativistic dof plus a two-component fermionic DM particle give rise to

$$g_{*\text{BH}} = 108.5 \quad e_T = 7.6 \times 10^{-3} \quad [T_{\text{BH}} > T_{\text{EW}}], \quad (2.5)$$

see App. A for more details. The effects of changing the number of dof, are explored in detail in App. C.

From eq. (2.3), the BH mass evolves with time as follows:

$$M_{\text{BH}}(t) = M_F \left(1 - \frac{(t - t_F)}{\tau} \right)^{1/3}, \quad (2.6)$$

with M_F the BH mass at formation, and t_F the time of formation. The BH lifetime, τ , reads

$$\tau = \frac{1}{3e_T} \frac{M_F^3}{M_p^4}. \quad (2.7)$$

Furthermore, by integrating eq. (2.2) over energy and time, we can also compute the total number of particle species j emitted over the PBH lifetime. In particular, for a fermionic species j , we have

$$N_j = g_j \frac{81\zeta(3)}{4096\pi^4 e_T} \frac{M_F^2}{M_p^2} = 3.2 \times 10^{-2} g_j \frac{M_F^2}{M_p^2} \quad [j \equiv \text{fermion}], \quad (2.8)$$

where we have used e_T from eq. (2.5) in the second equality.

The question that actually arises is what should we expect as initial mass M_F and formation time t_F . Here we assume that the inflaton decays into radiation with an overdensity on a suitably small scale. If this overdensity is larger than the equation of state parameter, $w = 1/3$, it will collapse into a PBH of mass

$$M_F = \gamma \rho_F \frac{4\pi}{3} H_F^{-3}, \quad (2.9)$$

where $H_F = 1/(2t_F)$ is the Hubble scale at PBH formation in a radiation era, and $\gamma \sim w^{3/2} \approx 0.2$ captures the efficiency of collapsing the overdense region into the PBH [47]. We can now use the Friedmann equation $H_F^2 = 8\pi\rho_F/(3M_p^2)$ to relate H_F to the total energy density at formation time, ρ_F ,

$$\rho_F = 3(4\pi\gamma)^2 M_F T_F^3, \quad (2.10)$$

where $T_F = M_p^2/(8\pi M_F)$ is the BH temperature at formation time. Hence, the time of formation is given by

$$t_F = \frac{M_F}{\gamma M_p^2}. \quad (2.11)$$

The constraint on the tensor-to-scalar ratio from the CMB limits the scale of inflation to $H_{\text{Inf}} \lesssim 10^{14} \text{ GeV}$ [48], and in turn, as $H_F < H_{\text{Inf}}$, the initial PBH mass should satisfy the lower bound:

$$M_F \gtrsim 10^4 M_p. \quad [\text{Inflation}] \quad (2.12)$$

Following the literature, we denote the initial PBH abundance as

$$\beta \equiv \Omega_{\text{PBH}}(t_F), \quad (2.13)$$

which allows us to express the initial PBH number density as

$$n_{\text{BH}}(t_F) = \frac{\beta}{M_F} \rho_F = 3\beta(4\pi\gamma)^2 T_F^3. \quad (2.14)$$

As fluctuations of the density contrast which exceed the threshold value $w = 1/3$ and collapse can be rare, not all Hubble patches at t_F will produce a PBH, and it is possible to have $\beta \ll 1$ [34]. After being produced in the radiation dominated era, the energy density of PBHs initially grows as

$$\Omega_{\text{BH}}(t) = \frac{\rho_{\text{BH}}(t)}{\rho_{\text{tot}}(t)} \propto a(t), \quad (2.15)$$

where ρ_{tot} is the total density, originally dominated by the radiation density ρ_R , and a is the scale factor. Provided they do not decay beforehand, we reach $\rho_{\text{BH}}/\rho_R \approx 1$ at the PBH-radiation equality time, t_{eq} . Assuming that $a(t) \propto t^{1/2}$ up to equality, we have

$$t_{\text{eq}} \simeq t_F/\beta^2. \quad (2.16)$$

In order for BHs to dominate the universe before evaporation – thus giving rise to an early matter dominated era – t_{eq} should be smaller than the evaporation time, $t_{\text{ev}} = t_F + \tau \simeq \tau$ (this is valid for the cases considered here, see below). Equivalently, we need $\beta > \beta_c$ with

$$\beta_c = \sqrt{\frac{3eT}{\gamma}} \frac{M_p}{M_F}. \quad (2.17)$$

Note that the temperature of the plasma surrounding the PBH at formation,

$$T(t_F) = \left(\sqrt{\frac{45}{16\pi^3 g_*(t_F)}} \frac{\gamma M_p^3}{M_F} \right)^{1/2}, \quad (2.18)$$

exceeds the BH temperature T_F . Hence, the PBHs do not start decaying immediately, but only at some later time, either when the plasma has cooled sufficiently, or when the PBHs grow to dominate the energy density, depending on which occurs first. In either case t_{ev} is still dominated by the PBH lifetime τ . The estimate of the efficiency of the Bondi accretion [49] onto the PBHs carries a large uncertainty, see e.g. [50–52]. Moreover, even if the accretion efficiency is close to unity, the corrections to the “initial” BH mass and τ are only of $\mathcal{O}(1)$ [35, 36]. We therefore do not include such effects in our study but keep in mind the possibility of some corrections if the accretion is indeed efficient.

3 Relic dark matter from evaporation

Sourcing the DM relic abundance from BH decay has been considered in a number of previous studies [28–37]. Given an initial BH mass, M_F , there generally exist two solutions to match onto the relic abundance, depending on whether the initial BH temperature, T_F , is above or below m_{DM} , see e.g. [31, 33]. In the case of $m_{\text{DM}} > T_F$, solutions exist with $m_{\text{DM}} < M_p$ for monochromatic mass functions with $M_F \gtrsim 10^9 M_p$. The DM ends up cold enough to not be subject to structure formation constraints [31] and will be of no further interest to us here.

We now proceed to estimate the relic abundance of light DM, $m_{\text{DM}} < T_F$, from PBH evaporation. Barring additional non-standard expansion, from evaporation time onward the DM rest energy density, $n_{\text{DM}} m_{\text{DM}}$, scales as a^{-3} , meaning that²

$$\Omega_{\text{DM}}(t_0) = \frac{m_{\text{DM}} n_{\text{DM}}(t_{\text{ev}})}{\rho_c} \times \left(\frac{a_{\text{ev}}}{a_0} \right)^3, \quad (3.1)$$

where $n_{\text{DM}}(t_{\text{ev}})$ is the DM number density at evaporation, ρ_c is the critical energy density today, and $a_0 \equiv 1$ is the scale factor today. We can write $n_{\text{DM}}(t_{\text{ev}}) = N_{\text{DM}} n_{\text{BH}}(t_{\text{ev}})$, where $n_{\text{BH}}(t_{\text{ev}})$ is the BH number density at evaporation time and N_{DM} is the total number of DM particles emitted by one PBH. This latter quantity is given in eq. (2.8) for fermionic DM.

Let us first evaluate the scale factor at evaporation. We use entropy conservation between evaporation and today³, i.e. $s_0 a_0^3 = s_{\text{ev}} a_{\text{ev}}^3$, where s_0 denotes the present day entropy density. Immediately after evaporation the universe is radiation dominated, meaning that

$$H^2 = \frac{8\pi}{3M_p^2} \rho_R(t_{\text{ev}}) = \frac{8\pi^3 g_*(t_{\text{ev}}) T_{\text{ev}}^4}{90 M_p^2}, \quad (3.2)$$

²Notice that light DM produced by PBH evaporation is relativistic at the time of evaporation and a large part of its total energy density is kinetic energy. However, the latter quantity redshifts fast enough in order to be neglected today, see Sec. 5.3 for a detailed analysis.

³The entropy is not necessarily conserved between PBH formation and evaporation: if $\beta > \beta_c$ the new relativistic plasma arising from the PBH gives rise to a non-negligible increase of entropy, see e.g. [53].

where $\rho_R(t_{\text{ev}})$ and T_{ev} are the radiation energy density and the temperature at evaporation. Now, depending on β , the universe was either matter dominated (MD) or radiation dominated (RD) before evaporation, giving rise to two different evaporation scale factors. The Hubble scale at evaporation is $H_{\text{ev}} = 1/(2t_{\text{ev}})$ for RD or $H_{\text{ev}} = 2/(3t_{\text{ev}})$ for MD. In either case, $T_{\text{ev}} \propto 1/\sqrt{t_{\text{ev}}}$. Then using $s_0 a_0^3 = s_{\text{ev}} a_{\text{ev}}^3$, we obtain for the RD ($\beta < \beta_c$) scale factor

$$\begin{aligned} a_{\text{ev}}^{\text{RD}} &= \left(\frac{45s_0}{2\pi^2 g_{*s}(t_{\text{ev}})} \right)^{1/3} \left(\frac{32\pi^3 g_*(t_{\text{ev}}) t_{\text{ev}}^2}{90M_p^2} \right)^{1/4} \\ &= 2.5 \times 10^{-31} \left(\frac{M_F}{M_p} \right)^{3/2}. \end{aligned} \quad (3.3)$$

where g_{*s} counts the effective entropic degrees of freedom, see App. D. The second equality is valid for $T_{\text{ev}} > T_{\text{EW}}$. For the MD case ($\beta > \beta_c$) we instead find a slightly different result:

$$a_{\text{ev}}^{\text{MD}} = \left(\frac{9}{16} \right)^{1/4} a_{\text{ev}}^{\text{RD}} = 2.2 \times 10^{-31} \left(\frac{M_F}{M_p} \right)^{3/2}. \quad (3.4)$$

Additionally, we can evaluate the PBH number density at evaporation time $n_{\text{BH}}(t_{\text{ev}})$ as a function of the PBH number density at formation, eq. (2.14), by determining the ratio of scale factors between evaporation and formation. Here, we assume that the number of dof does not change between PBH formation and evaporation. We relax this assumption in App. C. The simplest case is when the universe is dominated by radiation the whole time. Then the scale factor simply scales as $a(t) \propto t^{1/2}$ and

$$\frac{a(t_F)}{a(t_{\text{ev}})} = \left(\frac{t_F}{t_{\text{ev}}} \right)^{1/2} = \left(\frac{3e_T}{\gamma} \right)^{1/2} \frac{M_p}{M_F} \quad \text{if } \beta < \beta_c. \quad (3.5)$$

Alternatively, in the case where BHs can dominate the universe, the $a(t) \propto t^{1/2}$ dependence cannot be expected at all times between t_F and t_{ev} . A good estimate of the ratio can instead be obtained by assuming that $\rho_{\text{BH}}(t_{\text{ev}}) \approx \rho_R(t_{\text{ev}})$ and that $\rho_{\text{BH}} \propto a^{-3}$ between t_F and t_{ev} , effectively neglecting the loss in mass of the BH by assuming that it happens rather instantaneously around $t \simeq t_{\text{ev}}$. Using that $\rho_R(t_{\text{ev}}) = 3M_p^2/(8\pi) \times (2/(3t_{\text{ev}}))^2$, we can easily extract the following expression:

$$\frac{a(t_F)}{a(t_{\text{ev}})} = \left(\frac{16e_T^2}{\gamma^2 \beta} \frac{M_p^4}{M_F^4} \right)^{1/3} \quad \text{if } \beta > \beta_c. \quad (3.6)$$

Combining eq. (3.1) with eqs. (3.5)-(3.6), we find

$$\Omega_{\text{DM}}(t_0) = \frac{m_{\text{DM}} N_{\text{DM}} T_F^3}{\rho_c} \times \zeta_{\text{RD/MD}} \times \left(a_{\text{ev}}^{\text{RD/MD}} \right)^3, \quad (3.7)$$

where $\zeta_{\text{RD/MD}}$ is a RD or MD dependent reheating (RH) prefactor which reads

$$\zeta_{\text{RD/MD}} \simeq \begin{cases} 3 \beta (4\pi)^2 \gamma^{1/2} (3e_T)^{3/2} \frac{M_p^3}{M_F^3} & \text{if } \beta < \beta_c, \\ 3 (4\pi)^2 (4e_T)^2 \frac{M_p^4}{M_F^4} & \text{if } \beta > \beta_c. \end{cases} \quad (3.8)$$

Equivalently, using eqs. (3.3)-(3.4) with $T_{\text{ev}} > T_{\text{EW}}$, we have:

$$\frac{\Omega_{\text{DM}}(t_0)h^2}{0.12} = \left(\frac{m_{\text{DM}}}{1 \text{ MeV}}\right) \times \begin{cases} \left(\frac{M_F}{1.1 \times 10^7 M_p}\right)^{1/2} \left(\frac{\beta}{3.6 \times 10^{-8}}\right) & \text{if } \beta < \beta_c, \\ \left(\frac{M_F}{1.1 \times 10^7 M_p}\right)^{-1/2} & \text{if } \beta > \beta_c. \end{cases} \quad (3.9)$$

From the above result, it is clear that the DM abundance scales very differently with the initial PBH mass M_F depending if their initial density β is larger or smaller than the critical density. For $T_{\text{ev}} < T_{\text{EW}}$, the number of dof $g_*(t_{\text{ev}})$ decreases and slightly affects both a_{ev} and Ω_{DM} . For a detailed treatment, see App. C.

During the early matter dominated epoch, overdensities, defined as $\delta \equiv \rho/\rho_{\text{tot}} - 1$, will grow linearly with the scale factor if they are subhorizon scale. We assume such overdensities, at length scales much larger than the initial overdensity which lead to PBH formation, exist at a CMB-inspired level of $\delta_i \sim 10^{-5}$. These overdensities will grow until the PBHs decay into radiation, which includes our DM, whereupon the overdensity is efficiently suppressed provided it is in the linear regime [54–56]. Indeed, the decay into radiation leads to oscillations in the plasma which can be a source of gravitational waves if the PBH mass function is sufficiently narrow [57]. Therefore, we do not need to be concerned about additional structure formed due to the period of early matter domination as long as the overdensities do not enter the non-linear regime before evaporation. If they enter the non-linear regime, additional long-living structures such as larger PBHs could presumably be formed, although the dynamics are non-trivial. As our analyses do not take into account such non-linearities, the range of validity entails

$$\frac{\delta_{\text{ev}}}{\delta_i} = \frac{a(t_{\text{ev}})}{a(t_{\text{eq}})} \approx \left(\frac{\beta}{\beta_c}\right)^{4/3} < 10^5, \quad (3.10)$$

where δ_{ev} (δ_i) is the overdensity at evaporation (initial overdensity). In deriving the above we have used eq. (2.16), which implies $a(t_F)/a(t_{\text{eq}}) \approx \beta$, and eq. (3.6). Translating the above for convenience, our analysis will be valid for

$$\beta \lesssim 6 \times 10^3 \beta_c. \quad (3.11)$$

Independently of DM production and structure formation, we have to demand that the BHs evaporate before BBN, in order not to spoil agreement with observations [17, 21]. The precise limit depends on β but becomes very stringent below $T_{\text{ev}} \sim 4 \text{ MeV}$. In order to be safe, we impose a simplified constraint, that the temperature at evaporation $T_{\text{ev}} > 10 \text{ MeV} > T_{\text{BBN}}$. Making use of the Hubble rate and evaporation scale factors derived in this section, this translates into an upper bound on the initial BH mass,

$$M_F \lesssim 1.6 \times 10^{13} M_p \quad [\text{BBN}], \quad (3.12)$$

where we have used the number of relativistic dof at $T_{\text{ev}} = 10 \text{ MeV}$, $g_* = 10.75$.

4 Non-cold dark matter phase-space distribution

Light DM particles ($m_{\text{DM}} \ll T_{\text{BH}}$) emitted ultra-relativistically from PBH evaporation might leave a NCDM [58, 59] imprint on cosmological observables. In order to estimate this effect, we study in more detail the form of the momentum distribution. Here we will consider that the energy of the emitted particles is momentum dominated ($E \simeq p$). Using eq. (2.2) in this limit, and integrating over time between $t_F \simeq 0$ and τ , we can obtain the momentum distribution of particles of the species j arising from one BH at the time of evaporation, $dN_j/dp|_{t=t_{\text{ev}}}$.

A priori, one could distinguish two different scenarios, one in which the reheating would happen instantaneously after production, i.e. $t_F \sim \tau$, and a non-instantaneous reheating, in which case we should account for the redshifting of momenta of the emitted particles between t_F and τ with $\tau \gg t_F$. Given the lower bound on the BH mass from inflation, in eq. (2.12), we can easily check that the range of allowed BH masses always forces us to take into account the non-instantaneous reheating case, see App. B for details. Nonetheless, the case of instantaneous reheating allows to extract exact analytic results. Here, for the sake of completeness, we revisit the resulting velocity distribution for both cases in subsections 4.1 and 4.2. Our results fully agree with previous findings of [33], see Fig. 1.

Additionally we go one step further by deriving the resulting DM phase-space distribution, see Sec. 4.3, and interfacing it with a Boltzmann code, so as to extract a more precise imprint on the linear matter power spectrum, see Sec. 5. The public code CLASS [38, 58] allows the treatment of NCDM and involves the introduction of a NCDM temperature⁴

$$T_{\text{nCDM}}(t) = T_F \frac{a(t_{\text{ev}})}{a(t)}, \quad (4.1)$$

such that $T_F = T_{\text{nCDM}}(t_{\text{ev}})$. We also introduce the time-independent rescaled momentum variable

$$x(t) = \frac{p(t)}{T_{\text{nCDM}}(t)}, \quad (4.2)$$

which is nothing but the rescaled comoving momentum q of CLASS for NCDM particles. With these variables, we write the rescaled momentum distribution $dN_j/dx = g_j \xi \times \tilde{f}(x)$ with

$$\tilde{f}(x) = \frac{T_F^3}{M_p^2 g_j} \left. \frac{dN_j}{dp} \right|_{t=t_{\text{ev}}}, \quad (4.3)$$

where $\tilde{f}(x)$ is a universal momentum distribution, which is independent of the PBH mass, as will become clear in the next section, and the dimensionless coefficient is given by

$$\xi = \frac{M_p^2}{T_F^2}. \quad (4.4)$$

Furthermore, in order to provide an estimate of the typical mean velocity of the particle species j obtained from BH evaporation at evaporation time $t = t_{\text{ev}}$, we will evaluate

$$\langle p_j \rangle_{t=t_{\text{ev}}} = \frac{\int dx x \times T_F \tilde{f}(x)}{\int dx \tilde{f}(x)}. \quad (4.5)$$

⁴Notice that the parameter T_{nCDM} of CLASS is effectively a ratio of temperatures. In terms of the variables defined here, $T_{\text{nCDM}} = T_{\text{nCDM}}(t)/T(t_0) \times a(t)$, where $T(t_0)$ is the radiation temperature today. Let us emphasize that that $T_{\text{nCDM}}(t)$ is time dependent while T_{nCDM} is not.

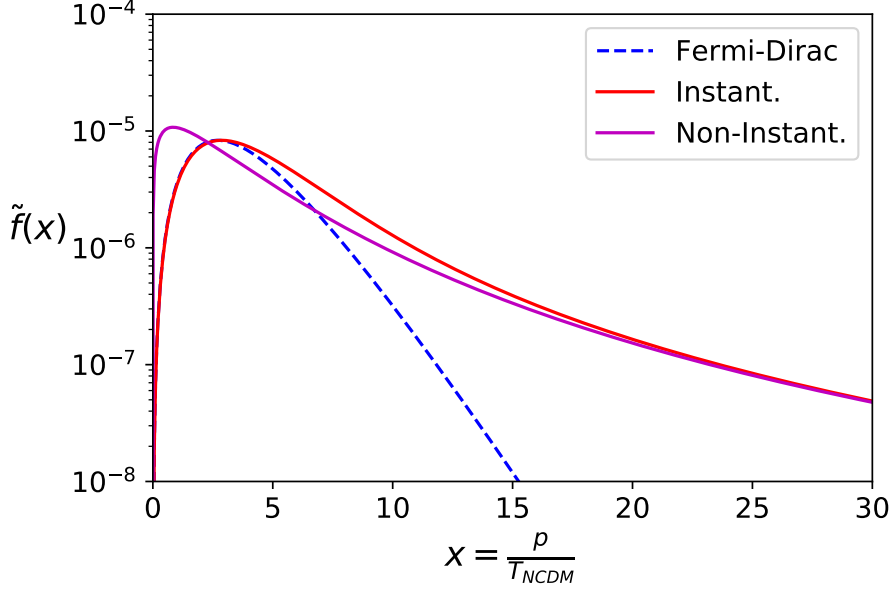


Figure 1. The continuous red and purple curves depict the universal NCDM momentum distribution $\tilde{f}(x)$ of eq. (4.3) arising from PBH evaporation as a function of the rescaled momentum x , assuming instantaneous and non-instantaneous reheating respectively. The dashed blue curve corresponds to a rescaled Fermi-Dirac distribution with a thermal body temperature $\tilde{T} = 1.3 \times T_F$. See Sec. 4.1 and Sec. 4.2 for details.

4.1 Instantaneous reheating

When considering instantaneous reheating, we expect that the particle momenta do not have time to be redshifted between the time of production and the end of reheating, so that the momentum distribution of particles of species j arising from a PBH reads

$$\left. \frac{dN_j}{dp} \right|_{t=t_{\text{ev}}} = \int_{t_F}^{t_{\text{ev}}} \frac{dN_j}{dp dt'}(p, t') dt'. \quad (4.6)$$

In practice, we know that $t_F \ll t_{\text{ev}}$ for the BH mass range of interest. In this context, integrating the instantaneous distribution of eq. (4.6) from $t_F \simeq 0$ to $t_{\text{ev}} \simeq \tau$, we can rewrite the momentum distribution for e.g. a fermionic species in terms of the universal distribution function

$$\tilde{f}(x) = \frac{F_0}{x^3} \int_0^x \frac{y^4}{\exp(y) + 1} dy \quad \text{with} \quad F_0 = \frac{15}{8\pi^5 g_{\text{BH}}}. \quad (4.7)$$

This function is manifestly independent of the BH mass. Also notice that the above integral can be expressed in terms of special functions:

$$\begin{aligned} \int_0^x \frac{y^4}{\exp(y) + 1} dy &= \frac{x^5}{5} - x^4 \log(1 + e^x) - 4x^3 \text{Li}_2(-e^x) + 12x^2 \text{Li}_3(-e^x) \\ &\quad - 24x \text{Li}_4(-e^x) + 24 \text{Li}_5(-e^x) + \frac{45}{2} \zeta(5), \end{aligned} \quad (4.8)$$

where Li_n are polylogarithms.

The universal distribution of eq. (4.7) for instantaneous reheating is shown as a function of the momentum x in Fig. 1 with a red continuous line. One can compare this distribution to a Fermi Dirac phase-space distribution f_{FD} . For reference, we also show the renormalised distribution $N_{\text{norm}}(p/\tilde{T})^2 f_{\text{FD}}(p, \tilde{T})$ with a blue dashed curve in Fig. 1. The thermal body temperature $\tilde{T} = 1.3 \times T_F$ and the normalisation factor N_{norm} were chosen so as to get the peak of the distributions at the same position. The thermal distribution and the distribution arising from PBH evaporation match very closely at low momenta, in particular around the position of its maximum. However, in the case of PBH evaporation we get a higher velocity tail than the distribution arising from a thermal body of temperature $1.3 \times T_F$. We can obtain an analytic form of the mean momentum at evaporation from instantaneous PBH evaporation using eq. (4.5):

$$\langle p_j \rangle|_{t=\tau} = \frac{14\pi^3}{1440\zeta(3)} \frac{M_p^2}{M_F} \approx 6.3 \times T_F, \quad (4.9)$$

in agreement with [34].

This can be compared to the mean momentum resulting from a FD thermal distribution. In the latter case, we have $\langle p_j \rangle_{\text{FD}} = \frac{7\pi^4}{180\zeta(3)} \approx 3\tilde{T}$, where \tilde{T} is the thermal body temperature, i.e. the mean momentum of NCDM arising from a PBH is higher than the one of thermal NCDM.

4.2 Non-instantaneous reheating

In the case of a non-instantaneous reheating, in which case momenta can redshift between the initial time and the time of evaporation, the momentum distribution can be computed using

$$\left. \frac{dN_j}{dp} \right|_{t=t_{\text{ev}}} = \int_0^\tau dt' \frac{a(\tau)}{a(t')} \times \frac{dN_j}{dp' dt'} \left(p \frac{a(\tau)}{a(t')}, t' \right). \quad (4.10)$$

A priori, one should solve the coupled set of Boltzmann equations giving rise to the Hubble rate dependence in ρ_{BH} and ρ_R so as to extract the time dependence of $a(t)$. However, assuming that the reheating period is dominated by a fluid of equation of state w throughout, the scale factors will scale as $a(t) = t^{2/(3(1+w))}$. One can check that considering $w = 0$ or $1/3$ induces only very small changes in the momentum distribution. Hence, we will use this approximation instead of solving the full system.

In Fig. 1 we show with a purple continuous curve the resulting universal distribution function assuming a MD era before RH for a fermionic species. It presents a peak at lower velocities than in the instantaneous case, while the high velocity tail is unaffected, as already observed in [33]. However, the area under the red and purple curves is the same, meaning that the number of particles emitted by one BH (obtained in eq. (2.8)) is independent of the fast/slow reheating, as one would expect. We can further extract the typical mean momentum associated to the non-instantaneous RH. For a fermionic species we get a mean momentum at evaporation of

$$\langle p_j \rangle|_{t=\tau} \approx T_F \times \begin{cases} 5.3 & \text{for } \beta < \beta_c, \\ 5.1 & \text{for } \beta > \beta_c, \end{cases} \quad (4.11)$$

i.e. (slightly) lower values than in the instantaneous case of eq. (4.9), even though the peak in the velocity distribution appears at a momentum lower by a factor of ~ 4 in the non-instantaneous reheating case.

4.3 NCDM phase-space distribution

We define the DM phase-space distribution f_{DM} as

$$g_{\text{DM}} f_{\text{DM}}(p, t) = \frac{dn_{\text{DM}}}{d^3p}, \quad (4.12)$$

where g_{DM} is the number of DM degrees of freedom; n_{DM} is the DM number density, scaling as a^{-3} from evaporation time; and p is the momentum, scaling as $1/a$. The f_{DM} arising from a distribution of PBHs that is peaked on a given BH mass can be expressed in terms of the momentum distributions derived above as

$$f_{\text{DM}}(p, t) d\Omega = \frac{1}{g_{\text{DM}}} \frac{n_{\text{BH}}(t)}{p(t)^3} x \left. \frac{dN_{\text{DM}}}{dx} \right|_{t=t_{\text{ev}}}, \quad (4.13)$$

where we have defined $n_{\text{BH}}(t) = n_{\text{BH}}(t_F)(a(t_F)/a(t))^3$. Making use of the BH number density at formation time of eq. (2.14), of the ratio of scale factors between formation and evaporation time of eqs. (3.5)-(3.6), and the universal momentum distribution of eq. (4.3), we can rewrite eq. (4.13) as

$$f_{\text{DM}}(p, t) d\Omega = \zeta_{\text{RD/MD}} \times \frac{\xi \tilde{f}(x)}{x^2}, \quad (4.14)$$

where the RD or MD dependent prefactor was defined in eq. (3.8). Notice that all the results of eqs. (3.6), (3.5), and (4.14) assume no changes in the number of relativistic dof available between t_F and t_{ev} .

5 The non-cold dark matter imprint

The DM arising from PBH evaporation might be fast enough so as to erase small scale structures. Constraints from such effects have already been estimated in several previous works using different methods, see e.g. [31, 33]. In this work, for the first time, we extract NCDM constraints by making use of the universal distributions obtained in Sec. 4.2 for the non-instantaneous reheating case and calculate the resulting matter power spectrum.

The main constraints will arise from the Lyman- α forest flux power spectrum, which probes hydrogen clouds at redshifts $2 \lesssim z \lesssim 6$, and has been shown to provide constraints on the matter power spectrum on small scales [60, 61]. However, these scales are in the highly non-linear regime, and as such require computationally expensive hydrodynamical N-body simulations, which are currently only available for a limited subclass of models [62]. To circumvent the need for new N-body simulations, in this paper we use CLASS to extract the linear matter power spectrum of our NCDM scenario and the corresponding transfer function, similar to what is usually done for thermal warm dark matter (WDM) models [39]. We will show that, even though the PBH evaporation distribution function can differ from a thermal WDM distribution (which would follow a FD distribution, depicted by the blue dashed curve in Fig. 1), the resulting transfer functions have a form similar to those of thermal WDM. In the same spirit as [39] – or more recently [59] – we will fit the resulting transfer functions with a minimal set of parameters, incorporated in the breaking scale. This constitutes one of our main results, and will allow us to extract Lyman- α constraints for our scenarios.

In addition, our NCDM can affect the effective number of relativistic degrees of freedom at the time of CMB emission or BBN, see also [35–37]. Again, making use of the distribution

function of Sec. 4, we extract the contribution to the effective number of relativistic non-photonic species, ΔN_{eff} , coming from the NCDM from PBH in full generality, i.e. without assuming that the NCDM is still relativistic at CMB or BBN time, following the approach of [63]. This treatment of ΔN_{eff} differs from the default implementation for NCDM in CLASS, and also from e.g. [35, 36], the results of which are valid assuming that the NCDM is relativistic at the CMB or BBN time. Nevertheless, we reach the conclusion that the resulting ΔN_{eff} constraints cannot currently provide any bound on the parameter space for a 2 dof fermionic DM.

5.1 Estimate for the Lyman- α constraint

Before going through the results arising from CLASS, we first provide an estimate of the velocity constraints following an approach similar to [31, 36]⁵. For this purpose, we make use of the typical mean momenta at the time of evaporation obtained in Sec. 4. The mean velocity today of NCDM particles arising from PBH evaporation (that have not yet virialised) should satisfy

$$\langle v \rangle|_{t=t_0} = a_{\text{ev}} \times \frac{\langle p \rangle|_{t=\tau}}{m_{\text{DM}}} = \left(\frac{\text{keV}}{m_{\text{DM}}} \right) \left(\frac{M_F}{M_p} \right)^{1/2} \times \begin{cases} 6.4 \times 10^{-7} & \text{for } \beta < \beta_c, \\ 5.5 \times 10^{-7} & \text{for } \beta > \beta_c, \end{cases} \quad (5.1)$$

assuming that the DM momentum redshifts as $\propto 1/a$ from the end of evaporation onwards. In eq. (5.1) we have used the scale factor of eqs. (3.3) and (3.4) assuming $T_F > T_{\text{EW}}$, and the mean momentum obtained in eq. (4.11) assuming non-instantaneous RH. Notice that the mean DM velocity today increases for increasing PBH mass, while the mean momentum at the time of evaporation is smaller for higher PBH mass, see eqs. (4.9) and (4.11). It is important to take into account the redshifting of the momenta (which scales with $a_{\text{ev}} \propto M_F^{3/2}$) at later times in order to get the relevant DM velocity dependence in the PBH mass.

This velocity can be compared to the one expected for thermal WDM particles that saturate the Lyman- α bound. The typical velocity today of thermal DM particles that decoupled while still being relativistic is estimated to be [5]

$$v_{\text{WDM}}|_{t=t_0} \approx 3.9 \times 10^{-8} \left(\frac{\text{keV}}{m_{\text{WDM}}} \right)^{4/3}. \quad (5.2)$$

Imposing that the mean velocity of eq. (5.1) does not exceed the WDM velocity of eq. (5.2), for a WDM mass saturating the Lyman- α bound, $m_{\text{WDM}}^{\text{Ly}-\alpha}$, we get the constraint

$$m_{\text{DM}} \gtrsim \left(\frac{m_{\text{WDM}}^{\text{Ly}-\alpha}}{\text{keV}} \right)^{4/3} \left(\frac{M_F}{M_p} \right)^{1/2} \times \begin{cases} 16 \text{ keV} & \text{for } \beta < \beta_c, \\ 14 \text{ keV} & \text{for } \beta > \beta_c. \end{cases} \quad (5.3)$$

We will see in Sec. 5.2 that a dedicated analysis agrees with this simple estimate up to a factor of ~ 3 . The dependence of the limits on the NCDM mass from PBH evaporation in $m_{\text{WDM}}^{\text{Ly}-\alpha}$ and M_F is also well recovered using CLASS together with the distribution functions of Sec. 4.

⁵Also see [33] for a somewhat different approach, which takes greater account of the phase-space distribution, although without calculating the power spectrum, as we shall do later.

5.2 Lyman- α constraints from the transfer function

We now make use of the non-instantaneous phase-space distributions obtained in Sec. 4, using them as an input for NCDM in the Boltzmann code CLASS⁶ and we extract the resulting matter power spectrum, assuming that the NCDM accounts for all the DM. In order to parametrise the small scale suppression of the matter power spectrum within a given NCDM model with respect to the equivalent CDM case, one can express the ratio between the CDM power spectrum, $P_{\text{CDM}}(k)$, and the power spectrum of some new DM species X , $P_X(k)$, in terms of the transfer function T_X , defined as

$$P_X(k) = P_{\text{CDM}}(k) T_X^2(k), \quad (5.4)$$

where k is the wavenumber. It has been shown that the NCDM $T^2(k)$ can usually be parametrised in terms of a finite set of parameters and physical inputs. In particular, in the thermal WDM case, Refs. [5, 39] use the following parametrisation to describe the transfer function:

$$T_X(k) = (1 + (\alpha_X k)^{2\mu})^{-5/\mu}, \quad (5.5)$$

where μ is a dimensionless exponent and α_X is the breaking scale. A more general parametrisation that can be applied to a larger set of NCDM models was also introduced in [59, 64, 65].

In the case of thermal WDM, Ref. [39] obtained a very good fit to the N-body simulations for $\mu = 1.12$ and

$$\alpha_{\text{WDM}} = 0.049 \left(\frac{m_{\text{WDM}}}{1 \text{ keV}} \right)^{-1.11} \left(\frac{\Omega_{\text{WDM}}}{0.25} \right)^{0.11} \left(\frac{h}{0.7} \right)^{1.22} h^{-1} \text{ Mpc}, \quad (5.6)$$

in terms of the WDM mass m_{WDM} . The analysis of Ref. [39], and more recently [40], obtained a bound of $m_{\text{WDM}} > 3.3 \text{ keV}$ and 10 keV at 95 % C.L., respectively, from Lyman- α flux observations. We note, however, that there are claims in the literature [41, 66] that these m_{WDM} bounds depend heavily on the assumptions made about the instantaneous temperature and pressure effects of the intergalactic medium. Indeed, when relaxing these assumptions [41] find a bound of $m_{\text{WDM}} > 1.9 \text{ keV}$ at 95 % C.L.. With this in mind, we will take the bound of

$$m_{\text{WDM}} > 3 \text{ keV} \quad (5.7)$$

as a conservative limit from Lyman- α on WDM, and the breaking scale saturating this bound is $\alpha_{\text{WDM}} = 1.3 \times 10^{-2} \text{ Mpc } h^{-1}$. Further improvements on this bound might arise with extremely large telescopes, see [67].

We find that the transfer function of eq. (5.5) with $\mu = 1.12$ provides a very good fit to NCDM from PBH evaporation for a large set of DM and PBH masses. The breaking scale α_{PBH} in these cases will then be parametrised as

$$\alpha_{\text{PBH}} = \left(\frac{m_{\text{DM}}}{1 \text{ eV}} \right)^{-0.83} \left(\frac{M_{\text{F}}}{M_{\text{p}}} \right)^{0.42} \times \begin{cases} 60.4 \text{ Mpc } h^{-1} & \text{if } \beta < \beta_c, \\ 53.2 \text{ Mpc } h^{-1} & \text{if } \beta > \beta_c, \end{cases} \quad (5.8)$$

in the case of non-instantaneous reheating with $\Omega_{\text{DM}} h^2 = 0.12$ today. We checked that the fit is valid for $1.5 \times 10^{-3} < \alpha_{\text{PBH}} \times h / \text{Mpc} < 0.5$ with a deviation of maximum 15 %. The same

⁶Notice that in CLASS, NCDM is assumed to be composed of a 2 dof species by default. As a result, we have implemented $\mathbf{f}_0 = 2 \times f_{\text{DM}}$, with \mathbf{f}_0 the NCDM phase-space distribution of CLASS and f_{DM} from eq. (4.14). In our simulations, we fix the parameter `deg_ncdm` of CLASS, counting the number of NCDM generations, to one. This amounts to one fermionic 2 dof DM species, i.e. in our notations, to take $g_{\text{DM}} = 2$.

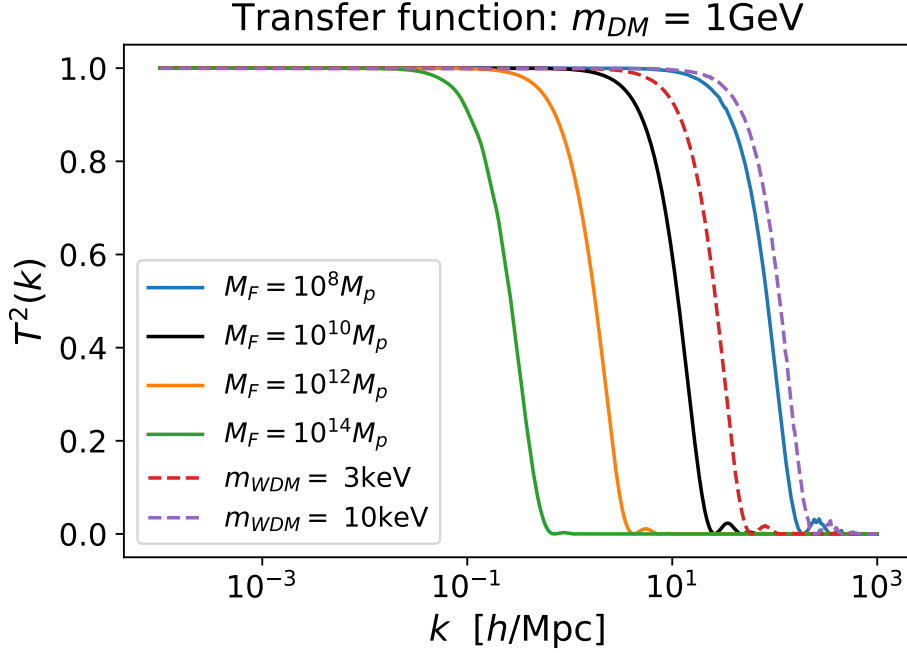


Figure 2. Transfer functions for NCDM from PBH non-instantaneous evaporation with $m_{\text{DM}} = 1 \text{ GeV}$ and $\beta > \beta_c$ (continuous lines) and WDM with $m_{\text{WDM}} = 3$ and 10 keV (red and purple dashed line respectively). The different coloured continuous lines correspond to different choices of PBH mass between $10^{14} M_p$ (left-most continuous green line) and $10^8 M_p$ (right-most continuous blue line). In all cases, it is assumed that the DM accounts for $\Omega_{\text{DM}} h^2 = 0.12$.

range of scales for α_{WDM} would correspond to $m_{\text{WDM}} \in [0.12, 22] \text{ keV}$, i.e. encapsulating the Lyman- α bound of eq. (5.7). If we had considered instantaneous RH, we would have a slightly larger breaking scale with prefactors of 68.2 (59.7) for $\beta < \beta_c$ ($\beta > \beta_c$). The dependency in m_{DM} and M_F is inspired by the analytic result of eq. (5.3). Indeed, imposing that the breaking scale in the PBH case should always be smaller than the breaking scale of WDM saturating the Lyman- α limit, we obtain a constraint on the mass of DM arising from PBH evaporation given by

$$m_{\text{DM}} \geq \left(\frac{m_{\text{WDM}}^{\text{Ly}-\alpha}}{\text{keV}} \right)^{4/3} \left(\frac{M_F}{M_p} \right)^{1/2} \times \begin{cases} 5.2 \text{ keV} & \text{if } \beta < \beta_c, \\ 4.4 \text{ keV} & \text{if } \beta > \beta_c. \end{cases} \quad (5.9)$$

The general result of eq. (5.8) can be used to model the effect of DM from PBHs on the matter power spectrum, and thus we can use this, together with eq. (5.9), to extract constraints from any small scale probe already testing the properties of thermal WDM.

In Fig. 2 we show some illustrative examples of transfer functions. The transfer function for a WDM candidate with $m_{\text{WDM}} = 3 \text{ keV}$, saturating our choice of conservative Lyman- α bound of eq. (5.7), and with $m_{\text{WDM}} = 10 \text{ keV}$, illustrating the currently most stringent bound of [40], are shown with dashed red and purple lines for comparison. In contrast, the continuous lines illustrate the case of NCDM with $m_{\text{DM}} = 1 \text{ GeV}$ arising from PBH evaporation for PBH masses between $10^{14} M_p$ (left-most continuous green line) and $10^8 M_p$ (right-most continuous blue line). In all cases, it has been assumed that the NCDM accounts for $\Omega_{\text{DM}} h^2 = 0.12$. The continuous lines have been obtained by using the DM phase-space

distributions of Sec. 4.3 assuming non-instantaneous RH with $\beta > \beta_c$, see Sec. 4.2. We see that for fixed NCDM mass, higher PBH mass imply higher velocities at the time of structure formation, see eq. (5.1) with $\langle v \rangle \propto M_F^{1/2}$, and thus an exponential cut in the transfer function arising at lower wave number k , or equivalently, at higher length scale. It is already well visible from Fig. 2 that a transfer function with similar parametrisation as the WDM will be able to describe NCDM from PBH evaporation. As a result, we can directly take away from Fig. 2 that, for $m_{\text{DM}} = 1 \text{ GeV}$, PBHs with mass $M_F < 10^{10} M_p$ are not allowed by the conservative Lyman- α bound of eq. (5.7), while the most stringent constraints from [40] would extend the exclusion to masses slightly below $M_F \sim 10^8 M_p$.

Let us emphasise that in Fig. 2, we always consider cases where the NCDM accounts for 100 % of the DM. The reason for this is that in mixed NCDM+CDM models, the transfer function presents a non-zero plateau at large k , which still contributes substantial power on small scales. As such, for these mixed cases the Lyman- α bounds need to be adjusted and this requires a dedicated analysis [68]. Thus, here we can only apply the bounds from Lyman- α when the NCDM accounts for all of the observed DM relic density today.

5.3 Contribution to ΔN_{eff}

The DM arising from PBH evaporation can also significantly contribute to the effective number of relativistic non-photon species, ΔN_{eff} , at the time of last scattering or BBN, provided the DM particles are relativistic enough at those times. Current CMB data tell us that $\Delta N_{\text{eff}}(t_{\text{CMB}}) < 0.28$ at 95 % C.L., using the latest measurements from the Planck collaboration (TT, TE, EE+lowE+lensing+BAO). Notice that the present tension in the Hubble constant measurement, can increase this upper bound to $\Delta N_{\text{eff}}(t_{\text{CMB}}) < 0.52$ at 95 % C.L. (TT, TE, EE+lowE+lensing+BAO+R18) [69]. Bounds of similar order are expected to arise from BBN measurements, see e.g. [70], keeping in mind that those bounds can be analysis-dependent, see e.g. [69, 71] for a discussion. These bounds are expected to improve by one order of magnitude with the upcoming CMB Stage IV mission, which is predicted to have a sensitivity of $\sigma(\Delta N_{\text{eff}}(t_{\text{CMB}})) \sim 0.06$ [72].

In order to evaluate the contribution to ΔN_{eff} , we have to carefully account for the fact that our DM is not always relativistic at the time of interest. We follow the approach of [63], see also e.g. [73]. The contribution from DM to $\Delta N_{\text{eff}}(T)$ at a given time, at SM radiation temperature T , is given by

$$\begin{aligned} \Delta N_{\text{eff}}(T) &= \frac{\rho_{\text{DM}}(T) - m_{\text{DM}} n_{\text{DM}}(T)}{\rho_{\text{rel } \nu}(T)/N_{\text{eff}}^{\nu}(T)} \\ &= \frac{g_{\text{DM}}}{2} \frac{30}{\pi^2} \frac{8}{7} \frac{T_{\text{nCDM}}(T)^4}{T^4} \left(\frac{T}{T_{\nu}} \right)^4 \zeta_{\text{RD/MD}} \frac{m_{\text{DM}}}{T_{\text{nCDM}}(T)} \\ &\quad \times \int dx \left(\left(1 + x^2 \frac{T_{\text{nCDM}}(T)^2}{m_{\text{DM}}^2} \right)^{1/2} - 1 \right) \xi \tilde{f}(x), \end{aligned} \quad (5.10)$$

see App. D for the details. In the second equality the RD-MD dependent prefactor is given by eq. (3.8). Notice that the ratio $(T/T_{\nu})^4$ evolves between BBN and today from 1 to $(11/4)^{4/3}$. One can easily check that the prefactor of x^2 in the integrand can be non-negligible for large PBH mass and low DM mass, e.g. $T_{\text{nCDM}}(t_{\text{CMB}})/m_{\text{DM}} = 1.32$ for $m_{\text{DM}} = 10^{-3} \text{ GeV}$ and $M_F = 10^{14} \times M_p$. In order to provide simple estimates of $\Delta N_{\text{eff}}(T)$, let us consider separately the highly relativistic and non-relativistic cases, i.e. the cases where the ratio $T_{\text{nCDM}}(T)/m_{\text{DM}}$ is much greater or smaller than one.

When $T_{\text{ncdm}}(T)/m_{\text{DM}} \gg 1$, the DM particles are still relativistic at the temperature T and eq. (5.10) simply reduces to

$$\Delta N_{\text{eff}}^{\text{rel}}(T) = \frac{120 \zeta_{\text{RD/MD}}}{7\pi^2} \left(\frac{T_F a_{\text{ev}}}{T_\nu a(T)} \right)^4 \frac{N_{\text{DM}} \langle p \rangle|_{t=\tau}}{T_F} \quad (5.11)$$

$$\simeq \frac{g_{\text{DM}}}{2} \begin{cases} 1.2 \times 10^{-1} \beta \times \frac{M_F}{M_p} & \text{if } \beta < \beta_c, \\ 4.1 \times 10^{-2} & \text{if } \beta > \beta_c. \end{cases} \quad (5.12)$$

In the second equality we make use of the fact that the product $(T/T_\nu)/(T \times a(T))$ is approximately constant between electron decoupling and today. We also use the results for a_{ev} , N_{DM} , and $\langle p \rangle|_{t=\tau}/T_F$ obtained in the previous sections. These results agree with the CLASS outputs that assumes by default that the NCDM component is relativistic. Furthermore, we find that in the PBH dominated case before evaporation, i.e. $\beta > \beta_c$, the $\Delta N_{\text{eff}}^{\text{rel}}$ contribution from DM arising from PBH evaporation does not depend on the PBH mass. This constant dependence agrees with the results of [35, 36]⁷. Comparing the $\beta > \beta_c$ results to the current bounds on ΔN_{eff} , it appears that current data are at the limit of restricting further the viable parameter space of a two dof fermionic DM species evaporating from PBH. In addition, when $\beta < \beta_c$, we typically have $\beta \times M_F/M_p < 0.3$ using eq. (2.17). As a result, for any β , we do not expect to get extra constraints on the viable DM parameter space making use of ΔN_{eff} constraints when considering $g_{\text{DM}} = 2$. Current CMB experiments would be able to test ΔN_{eff} for $\beta > \beta_c$ increasing the number of DM dof by a factor of ~ 7 , while future CMB experiments would just need a minor change in dof to test ΔN_{eff} .

Clearly, if relativistic DM does not enhance sufficiently N_{eff} to be constrained, we do not expect further bounds in the non-relativistic case. Indeed, when $T_{\text{ncdm}}(T)/m_{\text{DM}} \ll 1$, the ΔN_{eff} is no longer given by eq. (5.11) and the correctly computed contribution will always be smaller. Therefore, considering the relativistic result of eq. (5.11), as is the case in CLASS for example, might result in an over-constraining value for ΔN_{eff} . Nonetheless, for the sake of the discussion, let us briefly describe how the ΔN_{eff} contribution changes at a given time when the NCDM particles become non-relativistic. When $T_{\text{ncdm}}(T)/m_{\text{DM}} \ll 1$, eq. (5.10) tends to

$$\Delta N_{\text{eff}}^{\text{NR}}(T) = \frac{120 \zeta_{\text{RD/MD}}}{7\pi^2} \left(\frac{T_F a_{\text{ev}}}{T_\nu a(T)} \right)^4 \frac{N_{\text{DM}} \langle p^2 \rangle|_{t=\tau}}{T_F^2} \left(\frac{T_F a_{\text{ev}}}{2m_{\text{DM}} a(T)} \right). \quad (5.13)$$

Due to the non-relativistic nature of DM, its kinetic energy is expected to scale with the momentum squared $p^2/2m_{\text{DM}} \propto 1/a^2$ instead of $p \propto 1/a$. As a result, we are left with one negative power of the scale factor in the second line of eq. (5.13) that is not compensated by one negative power of the temperature T . In the non-relativistic case, we thus expect $\Delta N_{\text{eff}}(T)$ to differ between BBN and CMB epoch. In particular, at CMB time, we find:

$$N_{\text{eff}}^{\text{NR}}(T_{\text{CMB}}) = \frac{g_{\text{DM}}}{2} \frac{\langle p^2 \rangle|_{t=\tau}}{T_F^2} \left(\frac{\text{GeV}}{m_{\text{DM}}} \right) \begin{cases} 1.4 \times 10^{-12} \beta \left(\frac{M_F}{M_p} \right)^{3/2} & \text{if } \beta < \beta_c, \\ 8.6 \times 10^{-13} \left(\frac{M_F}{M_p} \right)^{1/2} & \text{if } \beta > \beta_c, \end{cases} \quad (5.14)$$

⁷We get similar results as in [35] for $\beta > \beta_c$. In the case $\beta < \beta_c$, we disagree in the PBH mass dependence of [35] but we agree with [36]. However, we trust that the dependence in eq. (5.12) is correct, as for $\beta = \beta_c$ we recover a mass independent result of the MD case.

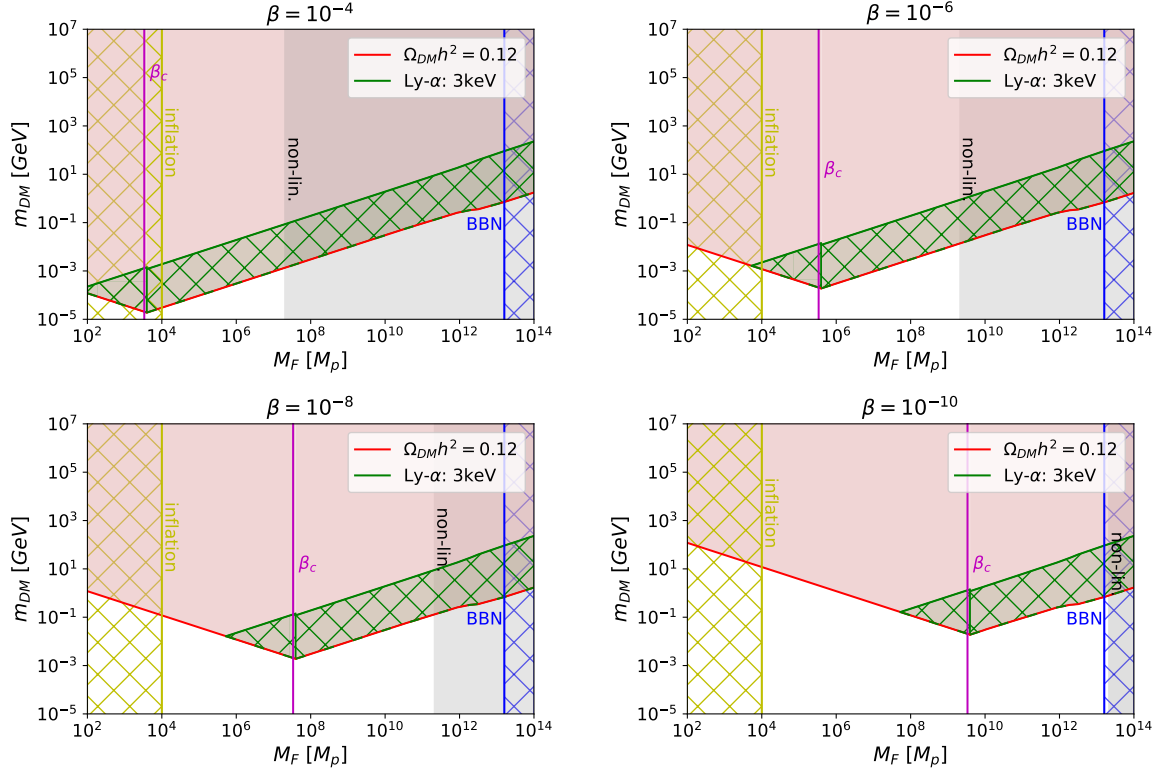


Figure 3. Viable parameter space for NCDM arising from PBH evaporation, for different values of β . The models on the red line produce the correct DM abundance today, while in the red region DM overcloses the universe. The blue, yellow, and green hatched zones are excluded by BBN, inflation, and Lyman- α constraints respectively, including where they overlap with the red line. In the grey region we do not fully trust our results as extra compact objects might have formed in the early MD era. The white regions show the viable parameter space that avoids all constraints.

where we expect $\langle p^2 \rangle|_{t=\tau}/T_F^2$, defined similarly as $\langle p \rangle|_{t=\tau}/T_F$, to be $\sim \mathcal{O}(10)$. At BBN we would obtain a result a factor of 4×10^6 larger (for $T_{BBN} = 4 \text{ MeV}$) if the particles were still non-relativistic at this earlier time. Even for the largest PBH masses and lowest DM masses considered here, the resulting $\Delta N_{\text{eff}}^{\text{NR}}$ is always left unconstrained.

6 Viable parameter space from cosmology

We can now summarise all the results obtained in the previous sections. For this purpose we show in Fig. 3 the viable parameter space in the plane (M_F, m_{DM}) for NCDM arising from PBH evaporation, for four different choices of the initial PBH relative abundance β . The initial black hole mass viable parameter space is bounded from above by the BBN constraint (blue hatched region), see eq. (3.12), and from below by inflation (yellow hatched region), see eq. (2.12). In the grey region we do not fully trust our results for DM production, as overdensities could have become non-linear and additional long-lived massive objects might have formed, see eq. (3.11).

The red line shows us where NCDM obtained from evaporation saturates the CMB bound on the DM relic abundance $\Omega_{\text{DM}} h^2 = 0.12$, in agreement with the CLASS result. Above the red line (light red region), PBHs produce too much DM and overclose the universe. The

$\Omega_{\text{DM}}h^2 = 0.12$ line changes slope for $\beta = \beta_c$, which is indicated with a magenta vertical line. On the left (right) of this line, the universe is RD (MD) before evaporation, i.e. $\beta < \beta_c$ ($\beta > \beta_c$) and the DM mass should decrease (increase) with increasing PBH mass in order to account for all the DM, as expected from the analytic results of eq. (3.9).

Notice that for PBH masses $M_F \gtrsim 10^{10}M_p$ the temperature of the bath at evaporation drops below T_{EW} . As a result, the number of SM relativistic dof at evaporation decreases: $g_*^{SM}(t_{\text{ev}}) < 106.75$, and the scale factor at evaporation will be affected, see eq. (3.5). The detailed impact of a change in the number of relativistic dof on the NCDM relic density is provided in App. C. The largest change happens for $\beta > \beta_c$, in which case $\Omega_{\text{DM}} \propto (g_*(t_{\text{ev}}))^{3/4}/g_{*s}(t_{\text{ev}})$, see eq. (C.7). For the largest PBH masses considered here, we expect $g_*^{SM}(t_{\text{ev}})$ to get as small as 10.75, implying a relic density larger by a factor of ~ 2 at most. As a result, for fixed M_F , m_{DM} will be reduced by up to a factor 2, explaining why the red curves scale down from $M_F \gtrsim 10^{10}M_p$.

The green line indicates where the Lyman- α bound, corresponding to a WDM of 3 keV, would exclude NCDM from PBH evaporation if this NCDM accounts for $\Omega_{\text{DM}}h^2 = 0.12$. We see that the Lyman- α bound only crosses the relic abundance line for $\beta < \beta_c$. Now any couple of (m_{DM}, M_F) giving rise to all the DM – i.e. any point on the red line – lying below the Lyman- α line would be excluded by any other bound on WDM excluding $m_{\text{WDM}} < 3$ keV. As a result, the Lyman- α bound excludes all scenarios giving rise to all the DM between the green line and the red line (green hatched region). Notice that NCDM with masses as large as 100 GeV can be excluded by this Lyman- α bound when arising from PBH evaporation.

For $M_F \gtrsim 10^{10}M_p$ the green line scales slightly up. This is again due to the change in the number of relativistic dof at evaporation that affect the scale factor a_{ev} , scaling as $g_*(t_{\text{ev}})^{1/4}/g_{*s}(t_{\text{ev}})^{1/3}$, entering in the determination of our Lyman- α bound. Going to lower PBH masses, we get lower $g_*(t_{\text{ev}})$ and slightly higher a_{ev} . Therefore, we expect from the analytic estimate of Sec. 5.1 that the NCDM velocity today will increase and the Lyman- α bound will be slightly reinforced. This is indeed observed in our simulations, see App. C. In particular, we use eq. (C.9) in our plots of Fig. 3.

Below the red line the Lyman- α bounds are no longer valid, as they were obtained assuming $\Omega_{\text{DM}}h^2 = 0.12$. If instead we consider that only part of the DM is made of NCDM, the form of the transfer function, and thus the Lyman- α bounds, drastically change. Getting the Lyman- α constraints in this region is non-trivial, see [66], and is beyond the scope of this paper. As such, we leave the region below the red line unconstrained, giving the possibility to account for part of the DM as NCDM from PBH evaporation.

In conclusion, we see that NCDM from PBH evaporation can still account for a sub-component of the DM for any β . By combining eqs. (3.9) and (5.9), we find the NCDM from PBH evaporation can account for all the DM when

$$\beta < 0.016 \beta_c. \quad (6.1)$$

For the lightest possible M_F this corresponds to $\beta \lesssim 5 \times 10^{-7}$ and $m_{\text{DM}} \gtrsim 2$ MeV. For larger M_F the allowed β (m_{DM}) decreases (increases). Such viable scenarios appear on the red line above the green region in the two bottom plots of Fig. 3.

7 Leptogenesis from PBH evaporation

Some words regarding baryogenesis are now in order. Although it has been speculated since the 1970s that PBHs may themselves be the seed for baryogenesis [27, 28, 31, 34, 74–89], we will limit ourselves to demanding the compatibility of our scenario with baryogenesis. If we assume our scenario produces the complete DM relic abundance, then we require eq. (6.1) to be satisfied. The PBHs produce a negligible entropy dump, and hence the scenario is entirely compatible with baryogenesis in general.

For example, let us consider the standard leptogenesis scenario in greater detail, assuming eq. (6.1) is satisfied. The heavy Majorana neutrinos will happily coexist in the plasma together with the PBHs and produce the baryon asymmetry through their CP violating decays in the standard way [90, 91]. Similarly, the PBH decay will only be affected in a negligible way by the emission of the Majorana neutrinos. Furthermore, it is possible to show that the neutrinos produced by the PBH will only contribute a negligible amount to the baryon asymmetry, outside of a tiny sliver of parameter space.

Let us examine the last point in greater detail⁸. Let us assume a hierarchical spectrum of heavy neutrinos and impose the Davidson-Ibarra bound on the CP violation in the decays of the heavy eigenstates [92]. Namely, the usual CP-violating parameter is bounded by

$$\epsilon \lesssim \frac{3M_N \delta m_\nu}{8\pi v_\phi^2}, \quad (7.1)$$

where $v_\phi = 246 \text{ GeV}$ is the electroweak VEV, M_N is the heavy neutrino mass, and finally $\delta m_\nu \sim 0.05 \text{ eV}$ is maximum difference in light neutrino masses. Although this constraint is usually applied to the lightest of the heavy mass eigenstates, the form of the CP violation [93] means similar arguments also hold for the heavier states.

To quantify, we can write the baryon yield from the heavy neutrinos emitted by the PBHs as [90, 91]

$$Y_B = \epsilon \kappa N_N Y_{\text{BH}}, \quad (7.2)$$

where $\kappa \simeq 28/79$ is the sphaleron reprocessing factor, N_N is the number of neutrinos emitted per PBH, and $Y_{\text{BH}} \equiv n_{\text{BH}}/s$ is the number density of PBHs normalised to the entropy density. The process is inherently out-of-equilibrium as T_{BH} exceeds the surrounding plasma temperature during the PBH decay process, thus satisfying the third Sakharov condition [76, 77]. The numerator of Y_{BH} at formation time, t_F , is given in eq. (2.14). The denominator follows immediately from eq. (2.18). In short $Y_{\text{BH}} \simeq 0.06 \beta (M_p/M_F)^{3/2}$. Finally we require N_N which can be found using eq. (2.8) assuming $M_N < T_F$. Note as $\epsilon \propto M_N$ and if $M_N > T_F$ the number $N_N \propto (M_p/M_N)^2$ [31], the maximum Y_B occurs when $M_N = T_F$, which we now impose. Realistically, for $M_N = T_F$ there is already a suppression in N_N , but an approximation is made here in order to find a conservative bound on Y_B . Combining all of the above, together with our Lyman- α constraint of eq. (6.1) for the DM arising from the PBH account for $\Omega h^2 = 0.12$, yields a limit

$$Y_B < 3.3 \times 10^{-4} \left(\frac{\delta m_\nu}{0.05 \text{ eV}} \right) \left(\frac{M_p}{M_F} \right)^{3/2}. \quad (7.3)$$

Comparing this with the observed asymmetry $Y_B^{\text{obs}} \simeq 0.86 \times 10^{-10}$ [69], in Fig. 4 we see that the PBH sourced neutrinos can contribute sizeably to the asymmetry only in a tiny

⁸Similar arguments have been made in [31], for $\beta > \beta_c$, and more generally in [34], which differs by not restricting the CP violation as we shall do.

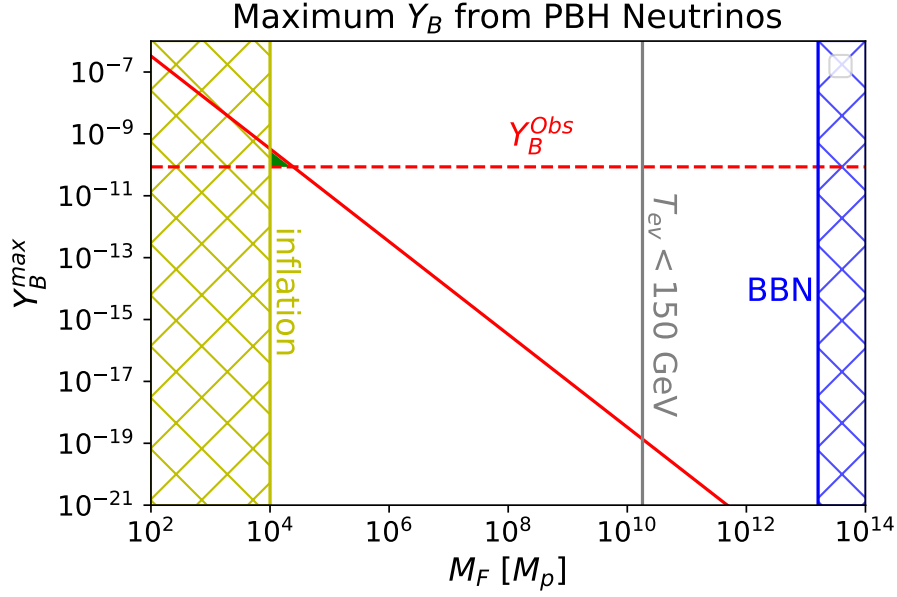


Figure 4. The red continuous line shows the maximum yield of baryons from decays of heavy neutrinos produced by PBHs in the standard leptogenesis scenario. This assumes that the NCDM produced by the PBH accounts for $\Omega_{\text{DM}}h^2 = 0.12$ and does not spoil Lyman- α constraints, see eq. (6.1). The observed asymmetry is shown as a dashed line. A further suppression, not taken into account here, occurs to the right of the grey vertical line due to the sphalerons switching off before the PBHs fully decay. The region of parameter space where the CP asymmetry could be accounted for is highlighted in green.

area of the parameter space highlighted in green, close to the bound coming from inflation. We re-emphasise that the heavy neutrinos in the bath can be more plentiful and hence still source the baryon asymmetry in the rest of the parameter space. Of course, in alternative scenarios the amount of CP violation can also be raised, which broadens the parameter space for which PBHs play a crucial role for baryogenesis.

8 Conclusions

In this paper we have revisited the case of NCDM particles arising from PBH evaporation. We do not assume any interaction for the DM except for gravitational interactions, and we focus on the production of DM particles with mass below the BH temperature at formation, $m_{\text{DM}} < T_F$. Such NCDM, not even feebly coupled to the SM, can leave a testable imprint on the cosmology by suppressing small scale structures, see e.g. [31–37] for previous analysis in this direction. We consider a Dirac-delta PBH mass distribution, having formed at the end of inflation in a radiation dominated era, with a proportion β normalised to the critical density. Depending on whether β is smaller or larger than some critical value β_c , the PBHs will evaporate in a radiation dominated or PBH dominated era. As already well-known, this directly affects the predictions for the NCDM relic abundance. Furthermore, PBH evaporation as such is already constrained by the allowed scale of inflation and should not spoil BBN. This constrains the BH mass at formation, M_F , to be in the range of $[10^4, 2 \times 10^{13}] \times M_p$.

Concerning the NCDM, we have fully accounted for the fact that the production at evaporation does not happen instantaneously. We have extracted the DM phase-space dis-

tribution and interfaced it with the public Boltzmann solver CLASS. We recover the DM relic abundance and find agreement with analytic estimates, independently of the instantaneous or non-instantaneous nature of the evaporation. In addition, we have updated the constraints arising from Lyman- α flux measurements. In particular, we have obtained a fit to the transfer functions arising from multiple simulations with CLASS, parametrised in terms of a single free parameter: the breaking scale α_{PBH} . The resulting fitting function appears to follow the very same parametrisation as the one for WDM in [39], even though the velocity distribution arising from PBH evaporation differs from a thermal distribution, displaying a higher velocity tail and a peak squeezed to lower velocities, see Fig. 1. The breaking scale α_{PBH} depends on M_F and m_{DM} , as specified in eq. (5.8). Imposing that α_{PBH} is smaller than the WDM breaking scale saturating the Lyman- α bounds gives us a generic constraint on the DM mass as a function of M_F in eq. (5.9). The resulting dependence agrees with analytic estimates we derived here, see also [31, 36].

We also computed the NCDM contribution to the number of non-photonic relativistic degrees of freedom ΔN_{eff} in full generality, i.e. not assuming beforehand that the DM is relativistic contrarily to e.g. CLASS, and provided simple analytic estimates for the extreme cases. We conclude that ΔN_{eff} does not further constrain the viable parameter space for our choice of NCDM with two fermionic dof. Future CMB missions will be on the verge of testing such contribution to ΔN_{eff} while increasing the number of DM dof by a factor of seven, current CMB constraints would already test ΔN_{eff} .

Our findings are summarised in the plots of Fig. 3 in the planes of (M_F, m_{DM}) for four different values of β . More generally, if a monochromatic distribution of PBHs came to dominate the energy density of the universe we find they cannot have decayed into light DM, $m_{DM} < T_F$, accounting for the complete relic abundance. On the other hand, if there is some other source of DM, we cannot quantify with the current method the fraction that could be NCDM from PBH evaporation, given that we can only apply the Lyman- α constraints to $\Omega_{DM} h^2 = 0.12$. We can also account for all the DM imposing a conservative Lyman- α bound corresponding to a $m_{WDM} = 3 \text{ keV}$ when satisfying eq. (6.1). Imposing the inflation bound, this implies that $\beta \lesssim 5 \times 10^{-7}$ and $m_{DM} \gtrsim 2 \text{ MeV}$. Notice that NCDM with mass as large as 100 GeV can be excluded by this Lyman- α bound when arising from PBH evaporation.

For the sake of completeness, we also revisit the possibility to account for both all the DM and for leptogenesis from heavy neutrinos arising from PBH. Taking into account the Lyman- α constraints derived here, maximising the baryon yield considering $M_N = T_F$, the PBH sourced neutrinos can only contribute sizeably to the asymmetry in a tiny area, close to the bound coming from inflation.

Acknowledgements

We would like to thank Sebastien Clesse for insightful discussion and Matteo Lucca for feedback on the draft. All the authors are supported by the Fonds National de la Recherche Scientifique (FRS-FNRS). IB is postdoctoral researcher of the FRS-FNRS with the project “*Exploring new facets of DM.*” QD, DCH, and LLH are (partially) supported by the FNRS research grant number F.4520.19. QD benefits from the support of the French community of Belgium through funding of a FRIA grant. LLH is a Research Associate of the FNRS and is also supported by the Vrije Universiteit Brussel through the Strategic Research Program *High-Energy Physics*.

A Greybody factors

We refer to the absorption probabilities $\Gamma_j(E, M_{\text{BH}})$, the coefficients entering in the evaluation of the number of particles per unit time and energy interval of eq. (2.2), as greybody factors. As mentioned in the text, these coefficients tend to the geometrical-optics limit – used in the bulk of the text – at high energy, but fall off more rapidly at low energy and this fall is spin-dependent. These greybody factors affect the power emitted by a black hole $-dM_{\text{BH}}/dt \sim \int dE E \Gamma_j$ and the number of emitted particles $dN/dt \sim \int dE \Gamma_j$ differently. They are also expected to affect the velocity distribution, shifting the maximum velocity peak to higher velocity, leading to a slight underestimation of the total portion of relativistic particles, as already underlined in [33].

When considering the geometrical-optics limit to compute the rate of BH mass loss, we obtain the result of eq. (2.3) involving a number of relativistic dof

$$g_{*\text{BH}} = \sum_b g_b + \sum_f \frac{7}{8} g_f, \quad (\text{A.1})$$

where $g_{j=b,f}$ counts all the bosonic and fermionic dof with mass smaller than the temperature of the BH. As mentioned in Sec. 2, accounting for all SM relativistic dof plus an extra two-component fermionic DM particle gives $g_{*\text{BH}} = 106.75 + 2 \times 7/8 = 108.5$ and $e_T = 7.6 \times 10^{-3}$.

The detailed computation of this mass loss rate, including the full treatment of the greybody factors, was obtained in [43, 94]. Following this prescription, the e_T factor of eq. (2.4) would become

$$\tilde{e}_T = \mathcal{G} \frac{\tilde{g}_{*\text{BH}}}{30720\pi} \quad \text{with} \quad \tilde{g}_{*\text{BH}} = \sum_i g_i X_i, \quad (\text{A.2})$$

for particles much lighter than the BH temperature, where $\mathcal{G} \simeq 3.8$, g_j denotes the number of dof and X_j encapsulates the spin-dependent greybody factor effect, see e.g. [35, 36]. In particular, a particle of spin 0, spin 1/2, or spin 1 would have $X_j = 1.82, 1.0, 0.41$ respectively. Considering again the emission of all the SM dof and 2 dof fermionic DM, Ref. [35] gets $\tilde{g}_{*\text{BH}} = 110$ and $\tilde{e}_T = 4.3 \times 10^{-3}$. The similarity between the numerical values of $g_{*\text{BH}}$ and $\tilde{g}_{*\text{BH}}$ is to be expected, as the SM is mainly made of fermions for which $X_i = 1.0$ in eq. (A.2), while they are weighted by 7/8 in eq. (A.1). Overall, neglecting the detailed effect of the greybody factors in computing the BH mass loss rate, we overestimate the latter by a factor ~ 2 , as e_T is approximatively twice as large as \tilde{e}_T . This also implies that the BH lifetime of eq. (2.7) is underestimated by a factor of 2. On the other hand, the number of emitted particles of species j is expected to scale as

$$\tilde{N}_j = g_j X'_j \frac{81\zeta(3)}{4096\pi^4 \tilde{e}_T} \frac{M_F^2}{M_p^2}, \quad (\text{A.3})$$

where the X'_j coefficient has yet to be determined and is expected to differ from X_j of eq. (A.2), as \tilde{N}_j and dM_{BH}/dt arise from different energy-dependent integrands involving Γ_j .

In the previous works evaluating the DM production from PBH evaporation, the detailed greybody factor impact on the emitted DM number of particles has been rather diverse, sometimes being omitted or partially taken into account, see e.g. refs. [28, 31–37]. Here for simplicity – and in order to provide a self-consistent analysis – we have chosen to use the geometrical-optics limit for the mass loss, the DM number density, and the impact on small

scale structure. We can, however, easily estimate how a change from e_T to \tilde{e}_T would affect the NCDM relic abundance modulo the uncertainty on X'_j in eq. (A.3). Indeed, the abundance scales as: $\Omega_{\text{DM}} \propto N_{\text{DM}} \times \zeta_{\text{RD/MD}} \times a_{\text{ev}}^3$, see eq. (3.7), while the number of DM particles from a BH, the scale factor at evaporation, and the prefactor $\zeta_{\text{RD/MD}}$ show the following dependencies in e_T : $N_{\text{DM}} \propto e_T^{-1}$, $a_{\text{ev}} \propto e_T^{-1/2}$ and $\zeta_{\text{RD/MD}} \propto e_T^{3/2}$ for $\beta < \beta_c$ or $\zeta_{\text{RD/MD}} \propto e_T^2$ for $\beta > \beta_c$, see eqs. (2.8), (3.3) and (3.4), and (3.8). As a result, a full treatment of the greybody factors will give rise to a NCDM relic density

$$\tilde{\Omega}_{\text{DM}}(t_0) = \Omega_{\text{DM}}(t_0) \times X'_{\text{DM}} \times \begin{cases} e_T/\tilde{e}_T & \text{if } \beta < \beta_c, \\ (e_T/\tilde{e}_T)^{1/2} & \text{if } \beta > \beta_c. \end{cases} \quad (\text{A.4})$$

where X'_{DM} is the prefactor X'_j in eq. (A.3) for $j = \text{DM}$ that would need to be computed, and $\Omega_{\text{DM}}(t_0)$ is the relic abundance in the geometrical-optics limit. For $T_{\text{ev}} > T_{\text{EW}}$, we thus expect $\tilde{\Omega}_{\text{DM}}(t_0)$ to differ from $\Omega_{\text{DM}}(t_0)$ by a factor $1.8 \times X'_{\text{DM}}$ for $\beta < \beta_c$ and a factor $1.3 \times X'_{\text{DM}}$ for $\beta > \beta_c$.

The impact of the full treatment of the greybody factors on the Lyman- α constraints depends both on the change in e_T , which affects a_{ev} , and on the expected shift of the peak in momentum of $dN(p)/dp$ to higher momenta, which would affect $\langle p \rangle|_{t=\tau}$. Here we can only derive the impact of the change in e_T on the breaking scale. Replacing e_T with \tilde{e}_T , we get the fitting formula

$$\alpha_{\text{PBH}} = \left(\frac{m_{\text{DM}}}{1 \text{ eV}} \right)^{-0.83} \left(\frac{M_{\text{F}}}{M_p} \right)^{0.42} \times \begin{cases} 74.7 \text{ Mpc } h^{-1} & \text{if } \beta < \beta_c, \\ 65.8 \text{ Mpc } h^{-1} & \text{if } \beta > \beta_c. \end{cases} \quad (\text{A.5})$$

This would imply a strengthening of the bounds obtained in Sec. 5.2 by $\sim 25\%$. The shift in the peak velocity to higher velocities would strengthen this bound even further.

B Validity of instantaneous evaporation approximation

In this appendix we derive under which conditions the instantaneous evaporation approximation is valid. Instantaneous evaporation takes place when

$$B^2 = \frac{H_F^{-2}}{\tau^2} \gg 1, \quad (\text{B.1})$$

with $H(t_F)$ the Hubble rate at formation [33]. It can easily be shown that in the BH production setup studied in this paper, the Hubble time at production is given by

$$H_F^{-1} = \frac{2M_F}{\gamma M_p^2}. \quad (\text{B.2})$$

As such, we obtain

$$B^2 = \frac{36e_T^2}{\gamma^2} \left(\frac{M_p^4}{M_F^4} \right) \leq \frac{36e_T^2}{\gamma^2} \frac{1}{10^{16}}, \quad (\text{B.3})$$

where we used the bound coming from inflation in eq. (2.12). Therefore, for the approximation to be valid we need to have $g_{*\text{BH}} \gtrsim 10^{10}$.

C Changing the number of degrees of freedom

In this appendix we generalise our results to take into account changing numbers of dof during the evaporation process. If the universe stays radiation dominated during evaporation, the ratio between the scale factor at formation and evaporation is given by

$$\frac{a_F}{a_{\text{ev}}} = \left(\frac{g_{*s}(t_{\text{ev}})}{g_{*s}(t_F)} \right)^{1/3} \left(\frac{g_*(t_F)}{g_*(t_{\text{ev}})} \right)^{1/4} \left(\frac{3\epsilon_T}{\gamma} \right)^{1/2} \left(\frac{M_p}{M_F} \right) \quad \text{if } \beta < \beta_c, \quad (\text{C.1})$$

following the same reasoning leading to eq. (3.5). It is clear that the above reduces to eq. (3.5) when the number of dof remains fixed.

In contrast, it turns out that the analogous ratio for $\beta < \beta_c$, eq. (3.6), is not affected by a change in dof, at least at the level of our approximation. To see this, we first require the entropy boost factor, D_s , due to PBH decay. At formation, the PBH density normalised to entropy is given by

$$Y_{\text{BH}}(t_F) \equiv \frac{n_{\text{BH}}(t_F)}{s(t_F)} = \beta \frac{\rho_R(t_F)}{M_F s(t_F)}. \quad (\text{C.2})$$

Precisely at the instant of evaporation, when the PBHs have reheated the thermal bath, the same factor is given by

$$Y_{\text{BH}}(t_{\text{ev}}) = \frac{\rho_R(t_{\text{ev}})}{M_F s(t_{\text{ev}})}, \quad (\text{C.3})$$

which implies

$$D_s = \frac{Y_{\text{BH}}(t_F)}{Y_{\text{BH}}(t_{\text{ev}})} = \beta \frac{g_*(t_F)}{g_*(t_{\text{ev}})} \frac{g_{*s}(t_{\text{ev}})}{g_{*s}(t_F)} \frac{T(t_F)}{T_{\text{ev}}}. \quad (\text{C.4})$$

The ratio of scale factors can then be written as

$$\frac{a_F}{a_{\text{ev}}} = \left[D_s \frac{s(t_F)}{s(t_{\text{ev}})} \right]^{1/3} = \left[\beta \frac{\rho_c(t_F)}{\rho_c(t_{\text{ev}})} \right]^{1/3} = \left(\frac{16e_T^2}{\gamma^2 \beta} \frac{M_p^4}{M_F^4} \right)^{1/3}. \quad (\text{C.5})$$

Here ρ_c denotes the critical density. To understand the result, note $\rho_c(t_F)$ can be written in terms of M_F , through eq. (2.10), in which the dof do not enter. Similarly, $\rho_c(t_{\text{ev}})$ is set by the Hubble scale at decay, and hence the PBH lifetime τ . Therefore, it depends on $g_{*\text{BH}}$ but not on the relativistic dof of the bath.

Taking these results into account, the prefactors of eq. (3.8), appearing in various quantities, become

$$\zeta_{\text{RD}} \rightarrow \left(\frac{g_{*s}(t_{\text{ev}})}{g_{*s}(t_F)} \right) \left(\frac{g_*(t_F)}{g_*(t_{\text{ev}})} \right)^{3/4} \zeta_{\text{RD}}, \quad \zeta_{\text{MD}} \rightarrow \zeta_{\text{MD}}. \quad (\text{C.6})$$

To understand the effect of changing the dof on the relic density we use eqs. (2.8), (3.1), (3.4), (C.1), and (C.6). This gives the following scaling

$$\Omega_{\text{DM}}(t_0) \propto \begin{cases} \frac{g_{\text{DM}} \times g_*(t_F)^{3/4}}{g_{*\text{BH}} \times g_{*s}(t_F)} & \text{if } \beta < \beta_c, \\ \frac{g_{\text{DM}} \times g_*(t_{\text{ev}})^{3/4}}{g_{*\text{BH}}^{1/2} \times g_{*s}(t_{\text{ev}})} & \text{if } \beta > \beta_c. \end{cases} \quad (\text{C.7})$$

A first interesting thing we notice from this is that in the case of $\beta < \beta_c$ the relic density is not influenced by the dof at evaporation, while in the case of $\beta > \beta_c$ the dof at formation do

not play a role. The results here are used in making the plots in Sec. 6, which result in small features in the contours at points where the SM dof change substantially.

As the scale factor at evaporation is altered by changing the dof, so is the free-streaming suppression. Keeping $g_{*s} = g_*$, the effects of a change in g_* and in g_{*BH} are captured by the following extra terms in the fitting formula for the breaking scale:

$$\alpha_{PBH} = \left(\frac{g_{*BH}}{108.5}\right)^{-0.42} \left(\frac{g_*(t_{ev})}{108.5}\right)^{-0.07} \left(\frac{m_{DM}}{1 \text{ eV}}\right)^{-0.83} \left(\frac{M_F}{M_p}\right)^{0.42} \times \begin{cases} 60.4 \text{ Mpc } h^{-1} & \text{if } \beta < \beta_c, \\ 53.2 \text{ Mpc } h^{-1} & \text{if } \beta > \beta_c. \end{cases} \quad (\text{C.8})$$

This implies that (5.9) becomes

$$m_{DM} \geq \left(\frac{g_{*BH}}{108.5}\right)^{-1/2} \left(\frac{g_*(t_{ev})}{108.5}\right)^{-1/12} \left(\frac{m_{WDM}^{\text{Ly}-\alpha}}{\text{keV}}\right)^{4/3} \left(\frac{M_F}{M_p}\right)^{1/2} \times \begin{cases} 5.2 \text{ keV} & \text{if } \beta < \beta_c, \\ 4.4 \text{ keV} & \text{if } \beta > \beta_c. \end{cases} \quad (\text{C.9})$$

The above dependence is inspired by our analytic estimates of Sec. 5 as the DM velocity is directly proportional to $a_{ev} \propto g_{*BH}^{-1/2} (g_*(t_{ev}))^{-1/12}$. Also notice that the effect of $g_*(t_{ev})$ is so suppressed by a small power that a large change in $g_*(t_{ev})$ would be needed to see a significant effect (above our error margin in the fits).

D Radiation contributions

The entropy is given by

$$s = \frac{2\pi^2}{45} g_{*s} T^3 \quad \text{with} \quad g_{*s} = \sum_b g_b \left(\frac{T_b}{T}\right)^3 + \sum_f \frac{7}{8} g_f \left(\frac{T_f}{T}\right)^3, \quad (\text{D.1})$$

where f and b count all the fermionic and bosonic relativistic dof and account for their temperature T_f , T_b relative to that of the thermal bath, T . The energy density of the relativistic particles is given by

$$\rho_R = \frac{\pi^2}{30} g_* T^4 \quad \text{and} \quad g_* = \sum_b g_b \left(\frac{T_b}{T}\right)^4 + \sum_f g_f \left(\frac{T_f}{T}\right)^4. \quad (\text{D.2})$$

Also notice that at $T \lesssim \text{MeV}$ the neutrinos are decoupled while still being non-relativistic. Using entropy conservation we can see that $\frac{T_\nu}{T} = \left(\frac{4}{11}\right)^{1/3}$ for $T \ll \text{MeV}$. When the temperature of the bath of photons T drops below $\sim \text{MeV}$, i.e. after e^+e^- decoupling, we use

$$g_*(T) = 2 \left(1 + \frac{7}{8} \left(\frac{T_\nu}{T}\right)^4 N_{\text{eff}}(T) \right) \quad [T \lesssim \text{MeV}]. \quad (\text{D.3})$$

In particular, around BBN we assume $T_\nu/T = 1$, while at the time of last scattering we have $T_\nu/T = (4/11)^{1/3}$. The first term in eq. (D.3) accounts for the photons, while the second

term accounts for the SM neutrinos and all other extra species that would still be relativistic today. Focusing on the SM only, one gets for $T < m_e$

$$g_{*,0}^{\text{SM}} \simeq 2 + 6 \frac{7}{8} \left(\frac{4}{11} \right)^{4/3} = 3.36 \quad \text{and} \quad g_{*,0}^{\text{SM}} \simeq 2 + 6 \frac{7}{8} \left(\frac{4}{11} \right)^{1/3} = 3.91, \quad (\text{D.4})$$

which implies the entropy today is $s_0 = 2.22 \times 10^{-38} \text{ GeV}^3$ using $T_0 = 2.7255 \text{ K}$. It is useful to remember that actually $N_{\text{eff}}^\nu = 3.046$ instead of $N_\nu/2 = 3$ for $T \ll m_e$, due to spectral distortions in the neutrino distribution function associated to non-instantaneous decoupling and flavour oscillations [95].

At this point, we can also define the contribution to N_{eff} from new dark degrees of freedom at a given temperature T . From eq. (D.3), we have that the dark degrees of freedom contribute as

$$\Delta N_{\text{eff}}(T) = \frac{\sum_D g_{*D} \left(\frac{T_D}{T} \right)^4}{2 \times \frac{7}{8} \left(\frac{T_\nu}{T} \right)^4} = \frac{\rho_{\text{rel}}^D(T)}{\rho_{\text{rel}}^{\text{SM}\nu}(T)/N_{\text{eff}}^\nu} = \frac{\rho_D(T) - \sum_D m_D n_D(T)}{\rho_{\text{rel}}^{\text{SM}\nu}(T)/N_{\text{eff}}^\nu}, \quad (\text{D.5})$$

i.e. $N_{\text{eff}} = N_{\text{eff}}^\nu + \Delta N_{\text{eff}}$. In the first line $g_{*D} = g_D$ for a boson and $g_{*D} = 7/8 \times g_D$ for a fermion, and g_D counts particle and antiparticle dof. In particular, for the case considered here, $g_{*DM} = \frac{7}{8} \times 2$ when the DM is relativistic. In the third equality we have interpreted the relativistic contribution of the dark species as their full contribution to the energy density $\rho \propto \int d^3p E f_D$, with $E^2 = p^2 + m_D^2$ minus the rest frame contribution, with $n_D \propto \int d^3p f_D$, where f_D is the dark species phase-space distribution, see [63, 73].

Finally, we note that the contribution from neutrinos at a given time is given by

$$\rho_{\text{rel}}^{\text{SM}\nu}(T) = 2 \times \frac{7}{8} \times N_{\text{eff}}^\nu \frac{\pi^2}{30} T^4 \left(\frac{T_\nu}{T} \right)^4. \quad (\text{D.6})$$

References

- [1] G. Arcadi, M. Dutra, P. Ghosh, M. Lindner, Y. Mambrini, M. Pierre et al., *The waning of the WIMP? A review of models, searches, and constraints*, *Eur. Phys. J. C* **78** (2018) 203 [[1703.07364](#)].
- [2] M. S. Pawlowski, B. Famaey, D. Merritt and P. Kroupa, *On the persistence of two small-scale problems in Λ CDM*, *Astrophys. J.* **815** (2015) 19 [[1510.08060](#)].
- [3] T. Sawala et al., *The APOSTLE simulations: solutions to the Local Group’s cosmic puzzles*, *Mon. Not. Roy. Astron. Soc.* **457** (2016) 1931 [[1511.01098](#)].
- [4] S. Tulin and H.-B. Yu, *Dark Matter Self-interactions and Small Scale Structure*, *Phys. Rept.* **730** (2018) 1 [[1705.02358](#)].
- [5] P. Bode, J. P. Ostriker and N. Turok, *Halo formation in warm dark matter models*, *Astrophys. J.* **556** (2001) 93 [[astro-ph/0010389](#)].
- [6] L. J. Hall, K. Jedamzik, J. March-Russell and S. M. West, *Freeze-In Production of FIMP Dark Matter*, *JHEP* **03** (2010) 080 [[0911.1120](#)].
- [7] X. Chu, T. Hambye and M. H. Tytgat, *The Four Basic Ways of Creating Dark Matter Through a Portal*, *JCAP* **05** (2012) 034 [[1112.0493](#)].
- [8] N. Bernal, M. Heikinheimo, T. Tenkanen, K. Tuominen and V. Vaskonen, *The Dawn of FIMP Dark Matter: A Review of Models and Constraints*, *Int. J. Mod. Phys. A* **32** (2017) 1730023 [[1706.07442](#)].

- [9] S. Heeba, F. Kahlhoefer and P. Stöcker, *Freeze-in production of decaying dark matter in five steps*, *JCAP* **1811** (2018) 048 [[1809.04849](#)].
- [10] P. Ivanov, P. Naselsky and I. Novikov, *Inflation and primordial black holes as dark matter*, *Phys. Rev. D* **50** (1994) 7173.
- [11] A. Kalaja, N. Bellomo, N. Bartolo, D. Bertacca, S. Matarrese, I. Musco et al., *From Primordial Black Holes Abundance to Primordial Curvature Power Spectrum (and back)*, [1908.03596](#).
- [12] Y. Ali-Haïmoud and M. Kamionkowski, *Cosmic microwave background limits on accreting primordial black holes*, *Phys. Rev. D* **95** (2017) 043534 [[1612.05644](#)].
- [13] V. Poulin, P. D. Serpico, F. Calore, S. Clesse and K. Kohri, *CMB bounds on disk-accreting massive primordial black holes*, *Phys. Rev. D* **96** (2017) 083524 [[1707.04206](#)].
- [14] MACHO collaboration, C. Alcock et al., *Experimental limits on the dark matter halo of the galaxy from gravitational microlensing*, *Phys. Rev. Lett.* **74** (1995) 2867 [[astro-ph/9501091](#)].
- [15] F. Capela, M. Pshirkov and P. Tinyakov, *Constraints on Primordial Black Holes as Dark Matter Candidates from Star Formation*, *Phys. Rev. D* **87** (2013) 023507 [[1209.6021](#)].
- [16] N. Bellomo, J. L. Bernal, A. Raccanelli and L. Verde, *Primordial Black Holes as Dark Matter: Converting Constraints from Monochromatic to Extended Mass Distributions*, *JCAP* **1801** (2018) 004 [[1709.07467](#)].
- [17] B. Carr, K. Kohri, Y. Sendouda and J. Yokoyama, *New cosmological constraints on primordial black holes*, *Phys. Rev. D* **81** (2010) 104019 [[0912.5297](#)].
- [18] B. Carr, K. Kohri, Y. Sendouda and J. Yokoyama, *Constraints on Primordial Black Holes*, [2002.12778](#).
- [19] S. W. Hawking, *Black hole explosions*, *Nature* **248** (1974) 30.
- [20] S. W. Hawking, *Particle Creation by Black Holes*, *Commun. Math. Phys.* **43** (1975) 199.
- [21] K. Kohri and J. Yokoyama, *Primordial black holes and primordial nucleosynthesis. 1. Effects of hadron injection from low mass holes*, *Phys. Rev. D* **61** (2000) 023501 [[astro-ph/9908160](#)].
- [22] V. Poulin, J. Lesgourgues and P. D. Serpico, *Cosmological constraints on exotic injection of electromagnetic energy*, *JCAP* **03** (2017) 043 [[1610.10051](#)].
- [23] P. Stöcker, M. Krämer, J. Lesgourgues and V. Poulin, *Exotic energy injection with ExoCLASS: Application to the Higgs portal model and evaporating black holes*, *JCAP* **03** (2018) 018 [[1801.01871](#)].
- [24] H. Poulter, Y. Ali-Haïmoud, J. Hamann, M. White and A. G. Williams, *CMB constraints on ultra-light primordial black holes with extended mass distributions*, [1907.06485](#).
- [25] M. Lucca, N. Schöneberg, D. C. Hooper, J. Lesgourgues and J. Chluba, *The synergy between CMB spectral distortions and anisotropies*, *JCAP* **02** (2020) 026 [[1910.04619](#)].
- [26] S. K. Acharya and R. Khatri, *CMB spectral distortions constraints on primordial black holes, cosmic strings and long lived unstable particles revisited*, *JCAP* **02** (2020) 010 [[1912.10995](#)].
- [27] A. D. Dolgov, P. D. Naselsky and I. D. Novikov, *Gravitational waves, baryogenesis, and dark matter from primordial black holes*, *Submitted to: Phys. Rev. D* (2000) [[astro-ph/0009407](#)].
- [28] D. Baumann, P. J. Steinhardt and N. Turok, *Primordial Black Hole Baryogenesis*, [hep-th/0703250](#).
- [29] G. Matsas, J. Montero, V. Pleitez and D. Vanzella, *Dark matter: The Top of the iceberg?*, in *Conference on Topics in Theoretical Physics II: Festschrift for A.H. Zimmerman*, 10, 1998, [hep-ph/9810456](#).
- [30] N. F. Bell and R. R. Volkas, *Mirror matter and primordial black holes*, *Phys. Rev. D* **59** (1999)

107301 [[astro-ph/9812301](#)].

- [31] T. Fujita, M. Kawasaki, K. Harigaya and R. Matsuda, *Baryon asymmetry, dark matter, and density perturbation from primordial black holes*, *Phys. Rev. D* **89** (2014) 103501 [[1401.1909](#)].
- [32] R. Allahverdi, J. Dent and J. Osinski, *Nonthermal production of dark matter from primordial black holes*, *Phys. Rev. D* **97** (2018) 055013 [[1711.10511](#)].
- [33] O. Lennon, J. March-Russell, R. Petrossian-Byrne and H. Tillim, *Black Hole Genesis of Dark Matter*, *JCAP* **1804** (2018) 009 [[1712.07664](#)].
- [34] L. Morrison, S. Profumo and Y. Yu, *Melanopogenesis: Dark Matter of (almost) any Mass and Baryonic Matter from the Evaporation of Primordial Black Holes weighing a Ton (or less)*, *JCAP* **1905** (2019) 005 [[1812.10606](#)].
- [35] D. Hooper, G. Krnjaic and S. D. McDermott, *Dark Radiation and Superheavy Dark Matter from Black Hole Domination*, *JHEP* **08** (2019) 001 [[1905.01301](#)].
- [36] I. Masina, *Dark matter and dark radiation from evaporating primordial black holes*, [2004.04740](#).
- [37] D. Hooper, G. Krnjaic, J. March-Russell, S. D. McDermott and R. Petrossian-Byrne, *Hot Gravitons and Gravitational Waves From Kerr Black Holes in the Early Universe*, [2004.00618](#).
- [38] D. Blas, J. Lesgourgues and T. Tram, *The Cosmic Linear Anisotropy Solving System (CLASS) II: Approximation schemes*, *JCAP* **07** (2011) 034 [[1104.2933](#)].
- [39] M. Viel, J. Lesgourgues, M. G. Haehnelt, S. Matarrese and A. Riotto, *Constraining warm dark matter candidates including sterile neutrinos and light gravitinos with WMAP and the Lyman-alpha forest*, *Phys. Rev. D* **71** (2005) 063534 [[astro-ph/0501562](#)].
- [40] N. Palanque-Delabrouille, C. Yèche, N. Schöneberg, J. Lesgourgues, M. Walther, S. Chabanier et al., *Hints, neutrino bounds and WDM constraints from SDSS DR14 Lyman- α and Planck full-survey data*, [1911.09073](#).
- [41] A. Garzilli, O. Ruchayskiy, A. Magalich and A. Boyarsky, *How warm is too warm? Towards robust Lyman- α forest bounds on warm dark matter*, [1912.09397](#).
- [42] J. M. Bardeen, B. Carter and S. W. Hawking, *The four laws of black hole mechanics*, *Comm. Math. Phys.* **31** (1973) 161.
- [43] J. H. MacGibbon and B. R. Webber, *Quark- and gluon-jet emission from primordial black holes: The instantaneous spectra*, *Phys. Rev. D* **41** (1990) 3052.
- [44] D. N. Page, *Particle emission rates from a black hole: Massless particles from an uncharged, nonrotating hole*, *Phys. Rev. D* **13** (1976) 198.
- [45] D. N. Page, *Particle Emission Rates from a Black Hole: Massless Particles from an Uncharged, Nonrotating Hole*, *Phys. Rev. D* **13** (1976) 198.
- [46] A. Arbey and J. Auffinger, *BlackHawk: A public code for calculating the Hawking evaporation spectra of any black hole distribution*, [1905.04268](#).
- [47] B. J. Carr, *The Primordial black hole mass spectrum*, *Astrophys. J.* **201** (1975) 1.
- [48] PLANCK collaboration, Y. Akrami et al., *Planck 2018 results. X. Constraints on inflation*, [1807.06211](#).
- [49] H. Bondi, *On spherically symmetrical accretion*, *Mon. Not. Roy. Astron. Soc.* **112** (1952) 195.
- [50] B. J. Carr and S. Hawking, *Black holes in the early Universe*, *Mon. Not. Roy. Astron. Soc.* **168** (1974) 399.
- [51] P. S. Custodio and J. Horvath, *The Evolution of primordial black hole masses in the radiation dominated era*, *Gen. Rel. Grav.* **34** (2002) 1895 [[gr-qc/0203031](#)].

- [52] R. Guedens, D. Clancy and A. R. Liddle, *Primordial black holes in brane world cosmologies: Accretion after formation*, *Phys. Rev. D* **66** (2002) 083509 [[astro-ph/0208299](#)].
- [53] A. Chaudhuri and A. Dolgov, *PBH evaporation, baryon asymmetry, and dark matter*, [2001.11219](#).
- [54] A. L. Erickcek and K. Sigurdson, *Reheating Effects in the Matter Power Spectrum and Implications for Substructure*, *Phys. Rev. D* **84** (2011) 083503 [[1106.0536](#)].
- [55] G. Barenboim and J. Rasero, *Structure Formation during an early period of matter domination*, *JHEP* **04** (2014) 138 [[1311.4034](#)].
- [56] C. Miller, A. L. Erickcek and R. Murgia, *Constraining nonthermal dark matter's impact on the matter power spectrum*, *Phys. Rev. D* **100** (2019) 123520 [[1908.10369](#)].
- [57] K. Inomata, M. Kawasaki, K. Mukaida, T. Terada and T. T. Yanagida, *Gravitational Wave Production right after Primordial Black Hole Evaporation*, [2003.10455](#).
- [58] J. Lesgourgues and T. Tram, *The Cosmic Linear Anisotropy Solving System (CLASS) IV: efficient implementation of non-cold relics*, *JCAP* **1109** (2011) 032 [[1104.2935](#)].
- [59] R. Murgia, A. Merle, M. Viel, M. Totzauer and A. Schneider, *"Non-cold" dark matter at small scales: a general approach*, *JCAP* **1711** (2017) 046 [[1704.07838](#)].
- [60] S. Ikeuchi, *The baryon clump within an extended dark matter region*, *Astrophysics and Space Science* **118** (1986) 509.
- [61] M. J. Rees, *Lyman absorption lines in quasar spectra: evidence for gravitationally-confined gas in dark minihaloes*, *Monthly Notices of the Royal Astronomical Society* **218** (1986) 25P [<http://oup.prod.sis.lan/mnras/article-pdf/218/1/25P/3010626/mnras218-025P.pdf>].
- [62] J. S. Bolton, E. Puchwein, D. Sijacki, M. G. Haehnelt, T.-S. Kim, A. Meiksin et al., *The Sherwood simulation suite: overview and data comparisons with the Lyman α forest at redshifts $2 \leq z \leq 5$* , *Mon. Not. Roy. Astron. Soc.* **464** (2017) 897 [[1605.03462](#)].
- [63] A. Merle and M. Totzauer, *keV Sterile Neutrino Dark Matter from Singlet Scalar Decays: Basic Concepts and Subtle Features*, *JCAP* **1506** (2015) 011 [[1502.01011](#)].
- [64] R. Murgia, V. Iršič and M. Viel, *Novel constraints on noncold, nonthermal dark matter from Lyman- α forest data*, *Phys. Rev. D* **98** (2018) 083540 [[1806.08371](#)].
- [65] M. Archidiacono, D. C. Hooper, R. Murgia, S. Bohr, J. Lesgourgues and M. Viel, *Constraining Dark Matter-Dark Radiation interactions with CMB, BAO, and Lyman- α* , *JCAP* **10** (2019) 055 [[1907.01496](#)].
- [66] J. Baur, N. Palanque-Delabrouille, C. Yèche, A. Boyarsky, O. Ruchayskiy, E. Armengaud et al., *Constraints from Ly- α forests on non-thermal dark matter including resonantly-produced sterile neutrinos*, *JCAP* **12** (2017) 013 [[1706.03118](#)].
- [67] J. D. Simon et al., *Testing the Nature of Dark Matter with Extremely Large Telescopes*, [1903.04742](#).
- [68] A. Boyarsky, J. Lesgourgues, O. Ruchayskiy and M. Viel, *Lyman-alpha constraints on warm and on warm-plus-cold dark matter models*, *JCAP* **05** (2009) 012 [[0812.0010](#)].
- [69] PLANCK collaboration, N. Aghanim et al., *Planck 2018 results. VI. Cosmological parameters*, [1807.06209](#).
- [70] C. Pitrou, A. Coc, J.-P. Uzan and E. Vangioni, *Precision big bang nucleosynthesis with improved Helium-4 predictions*, *Phys. Rept.* **754** (2018) 1 [[1801.08023](#)].
- [71] N. Schöneberg, J. Lesgourgues and D. C. Hooper, *The BAO+BBN take on the Hubble tension*, *JCAP* **10** (2019) 029 [[1907.11594](#)].
- [72] K. Abazajian et al., *CMB-S4 Science Case, Reference Design, and Project Plan*, [1907.04473](#).

- [73] S. Baumholzer, V. Brdar, P. Schwaller and A. Segner, *Shining Light on the Scotogenic Model: Interplay of Colliders, Cosmology and Astrophysics*, [1912.08215](#).
- [74] B. J. Carr, *Some cosmological consequences of primordial black-hole evaporations*, *Astrophys. J.* **206** (1976) 8.
- [75] Y. Zeldovich, *Charge Asymmetry of the Universe Due to Black Hole Evaporation and Weak Interaction Asymmetry*, *Pisma Zh. Eksp. Teor. Fiz.* **24** (1976) 29.
- [76] D. Toussaint, S. B. Treiman, F. Wilczek and A. Zee, *Matter - Antimatter Accounting, Thermodynamics, and Black Hole Radiation*, *Phys. Rev. D* **19** (1979) 1036.
- [77] A. Dolgov, *Baryon asymmetry of the universe and violation of the thermodynamic equilibrium*, *Pisma Zh. Eksp. Teor. Fiz.* **29** (1979) 254.
- [78] M. S. Turner and D. N. Schramm, *The Origin of Baryons in the Universe and the Astrophysical Implications*, *Nature* **279** (1979) 303.
- [79] M. S. Turner, *Baryon production by primordial black holes*, *Phys. Lett.* **89 B** (1979) 155.
- [80] A. D. Dolgov, *Hiding of the conserved (anti)-baryonic charge into black holes*, *Phys. Rev. D* **24** (1981) 1042.
- [81] J. D. Barrow, E. J. Copeland, E. W. Kolb and A. R. Liddle, *Baryogenesis in extended inflation. 2. Baryogenesis via primordial black holes*, *Phys. Rev. D* **43** (1991) 984.
- [82] A. S. Majumdar, P. Das Gupta and R. P. Saxena, *Baryogenesis from black hole evaporation*, *Int. J. Mod. Phys. D* **4** (1995) 517.
- [83] N. Upadhyay, P. Das Gupta and R. P. Saxena, *Baryogenesis from primordial black holes after electroweak phase transition*, *Phys. Rev. D* **60** (1999) 063513 [[astro-ph/9903253](#)].
- [84] E. V. Bugaev, M. G. Elbakidze and K. V. Konishchev, *Baryon asymmetry of the universe from evaporation of primordial black holes*, *Phys. Atom. Nucl.* **66** (2003) 476 [[astro-ph/0110660](#)].
- [85] A. Hook, *Baryogenesis from Hawking Radiation*, *Phys. Rev. D* **90** (2014) 083535 [[1404.0113](#)].
- [86] T. Banks and W. Fischler, *CP Violation and Baryogenesis in the Presence of Black Holes*, [1505.00472](#).
- [87] Y. Hamada and S. Iso, *Baryon asymmetry from primordial black holes*, *PTEP* **2017** (2017) 033B02 [[1610.02586](#)].
- [88] B. Carr, S. Clesse and J. García-Bellido, *Primordial black holes, dark matter and hot-spot electroweak baryogenesis at the quark-hadron epoch*, [1904.02129](#).
- [89] J. García-Bellido, B. Carr and S. Clesse, *A common origin for baryons and dark matter*, [1904.11482](#).
- [90] W. Buchmuller, R. Peccei and T. Yanagida, *Leptogenesis as the origin of matter*, *Ann. Rev. Nucl. Part. Sci.* **55** (2005) 311 [[hep-ph/0502169](#)].
- [91] S. Davidson, E. Nardi and Y. Nir, *Leptogenesis*, *Phys. Rept.* **466** (2008) 105 [[0802.2962](#)].
- [92] S. Davidson and A. Ibarra, *A Lower bound on the right-handed neutrino mass from leptogenesis*, *Phys. Lett. B* **535** (2002) 25 [[hep-ph/0202239](#)].
- [93] L. Covi, E. Roulet and F. Vissani, *CP violating decays in leptogenesis scenarios*, *Phys. Lett. B* **384** (1996) 169 [[hep-ph/9605319](#)].
- [94] J. H. MacGibbon, *Quark- and gluon-jet emission from primordial black holes. ii. the emission over the black-hole lifetime*, *Phys. Rev. D* **44** (1991) 376.
- [95] G. Mangano, G. Miele, S. Pastor, T. Pinto, O. Pisanti and P. D. Serpico, *Relic neutrino decoupling including flavor oscillations*, *Nucl. Phys. B* **729** (2005) 221 [[hep-ph/0506164](#)].